

# Supplementary Material

## New Cyclic pentapeptides from the Mangrove-derived

### *Aspergillus fumigatus* GXIMD 03099

Yu Wang<sup>1,2,†</sup>, Guangping Cao<sup>1,2,†</sup>, Yuman Gan<sup>1,2</sup>, Xiao Lin<sup>1,2</sup>, Xiangxi Yi<sup>1,2</sup>, Longyan Zhao<sup>1,2</sup>, Yonghong Liu<sup>1,2</sup>, Chenghai Gao<sup>1,2,\*</sup>, and Meng Bai<sup>1,2,\*</sup>

<sup>1</sup> Guangxi Key Laboratory of Marine Drugs, Guangxi University of Chinese Medicine, Nanning 530200, China

<sup>2</sup> Institute of Marine Drugs, Guangxi University of Chinese Medicine, Nanning 530200, China

\* Correspondence: gaoch@gxtcmu.edu.cn (C.G.); XXBai2014@163.com.

† These authors contributed equally to this work.

**Abstract:** Four new cyclic pentapeptides, avellanins D–G (**1–4**), together with four known compounds (**5–8**), were isolated from a mangrove-derived *Aspergillus fumigatus* GXIMD 03099 fungus from *Acanthus ilicifolius* L. Their structures were elucidated by analysis of HRESIMS, NMR, and ESI-MS/MS data. Their absolute configurations were determined by X-ray diffraction analysis and Marfey's method. Compounds **1–8** were screened for insecticidal and antibacterial activities. Compound **2** showed insecticidal activity against newly hatched larvae of *Culex quinquefasciatus* with an LC<sub>50</sub> value of 86.6  $\mu$ M; compound **4** had weak activity against *Vibrio harveyi* with an MIC value of 5.85  $\mu$ M.

## List of Supporting Information

Figure S1. HPLC and UV spectra of *Aspergillus fumigatus* GXIMD 03099.

Figure S2.  $^1\text{H}$  NMR ( $\text{DMSO-}d_6$ , 500 MHz) spectrum of **1**.

Figure S3.  $^{13}\text{C}$  NMR ( $\text{DMSO-}d_6$ , 125 MHz) spectrum of **1**.

Figure S4. DEPT ( $\text{DMSO-}d_6$ , 125 MHz) spectrum of **1**.

Figure S5. HMQC spectrum of **1**.

Figure S6. HMBC spectrum of **1**.

Figure S7.  $^1\text{H}$ - $^1\text{H}$  COSY spectrum of **1**.

Figure S8. NOESY spectrum of **1**.

Figure S9. HR-ESI-MS spectrum of **1**.

Figure S10. ESI-MS/MS spectrum of **1**.

Figure S11. Marfey's analysis of **1**.

Figure S12. CD spectrum of **1** in MeOH.

Figure S13.  $^1\text{H}$  NMR ( $\text{DMSO-}d_6$ , 400 MHz) spectrum of **2**.

Figure S14.  $^{13}\text{C}$  NMR ( $\text{DMSO-}d_6$ , 100MHz) spectrum of **2**.

Figure S15. DEPT ( $\text{DMSO-}d_6$ , 100 MHz) spectrum of **2**.

Figure S16. HMQC spectrum of **2**.

Figure S17. HMBC spectrum of **2**.

Figure S18.  $^1\text{H}$ - $^1\text{H}$  COSY spectrum of **2**.

Figure S19. NOESY spectrum of **2**.

Figure S20. HR-ESI-MS spectrum of **2**.

Figure S21. ESI-MS/MS spectrum of **2**.

Figure S22. Marfey's analysis of **2**.

Figure S23. CD spectrum of **2** in MeOH.

Figure S24.  $^1\text{H}$  NMR ( $\text{DMSO-}d_6$ , 500 MHz) spectrum of **3**.

Figure S25.  $^{13}\text{C}$  NMR ( $\text{DMSO-}d_6$ , 125 MHz) spectrum of **3**.

Figure S26. DEPT ( $\text{DMSO-}d_6$ , 125 MHz) spectrum of **3**.

Figure S27. HMQC spectrum of **3**.

Figure S28. HMBC spectrum of **3**.

Figure S29.  $^1\text{H}$ - $^1\text{H}$  COSY spectrum of **3**.

Figure S30. NOESY spectrum of **3**.

Figure S31. HR-ESI-MS spectrum of **3**.

Figure S32. ESI-MS/MS spectrum of **3**.

Figure S33. Marfey's analysis of **3**.

Figure S34. CD spectrum of **3** in MeOH.

Figure S35.  $^1\text{H}$  NMR ( $\text{CD}_3\text{OD}$ , 500 MHz) spectrum of **4**.

Figure S36.  $^{13}\text{C}$  NMR ( $\text{CD}_3\text{OD}$ , 125 MHz) spectrum of **4**.

Figure S37. DEPT ( $\text{CD}_3\text{OD}$ , 125 MHz) spectrum of **4**.

Figure S38. HMQC spectrum of **4**.

Figure S39. HMBC spectrum of **4**.

Figure S40.  $^1\text{H}$ - $^1\text{H}$  COSY spectrum of **4**.

Figure S41. NOESY spectrum of **4**.

Figure S42. HR-ESI-MS spectrum of **4**.

Figure S43. ESI-MS/MS spectrum of **4**.

Figure S44. Marfey's analysis of **4**.

Figure S45. CD spectrum of **4** in MeOH.

Crystal data and structure refinement for **5**

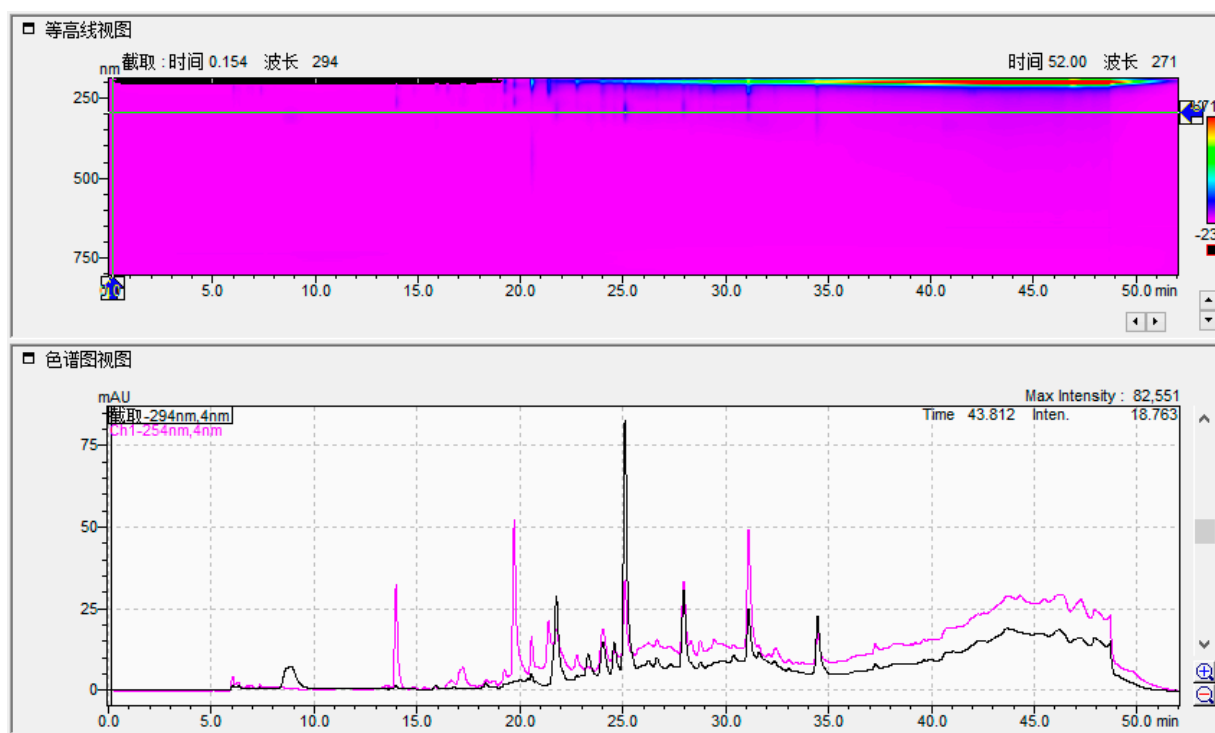


Figure S1. HPLC and UV spectra of *Aspergillus fumigatus* GXIMD 03099.

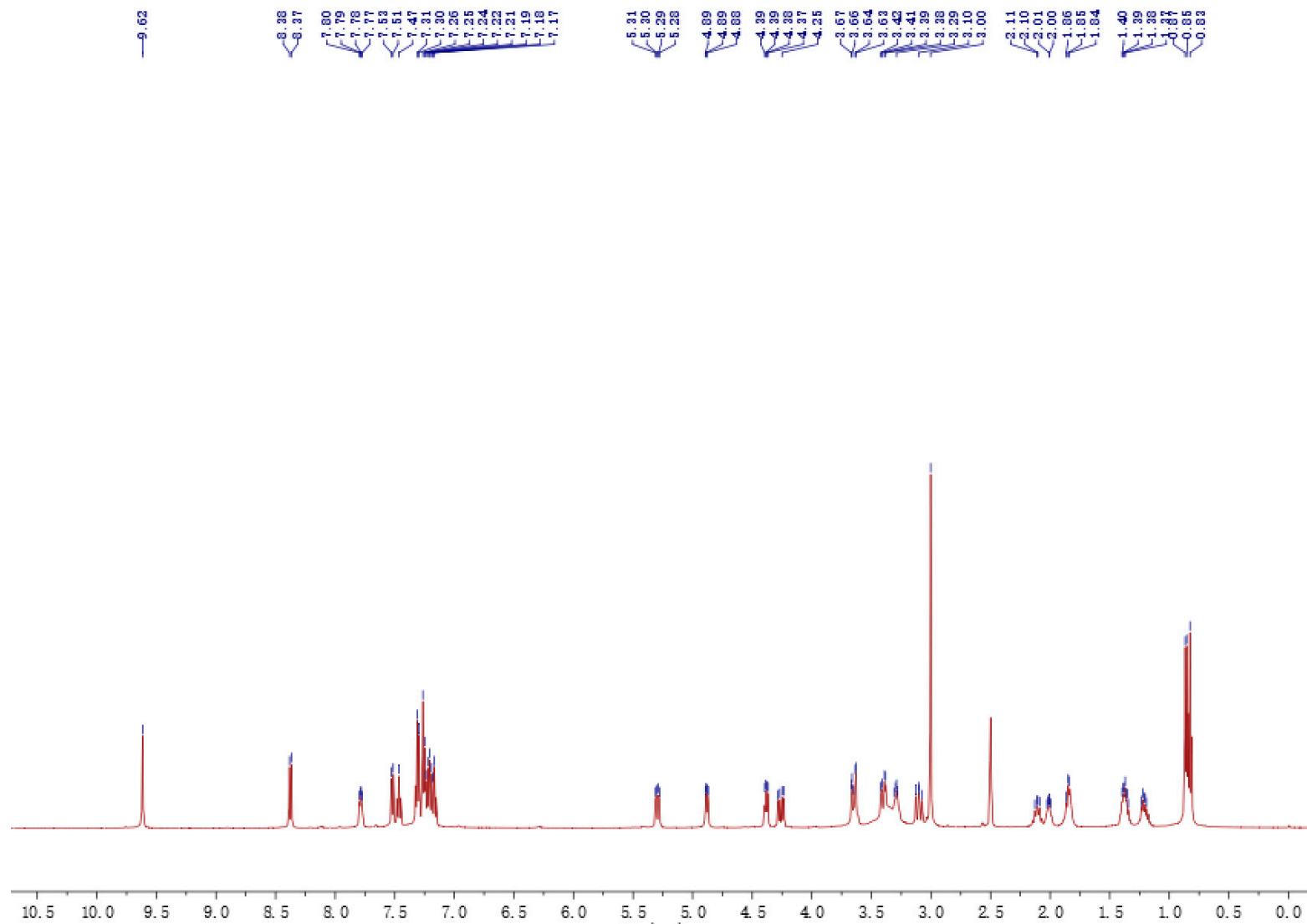


Figure S2.  $^1\text{H}$  NMR ( $\text{DMSO-}d_6$ , 500 MHz) spectrum of **1**.

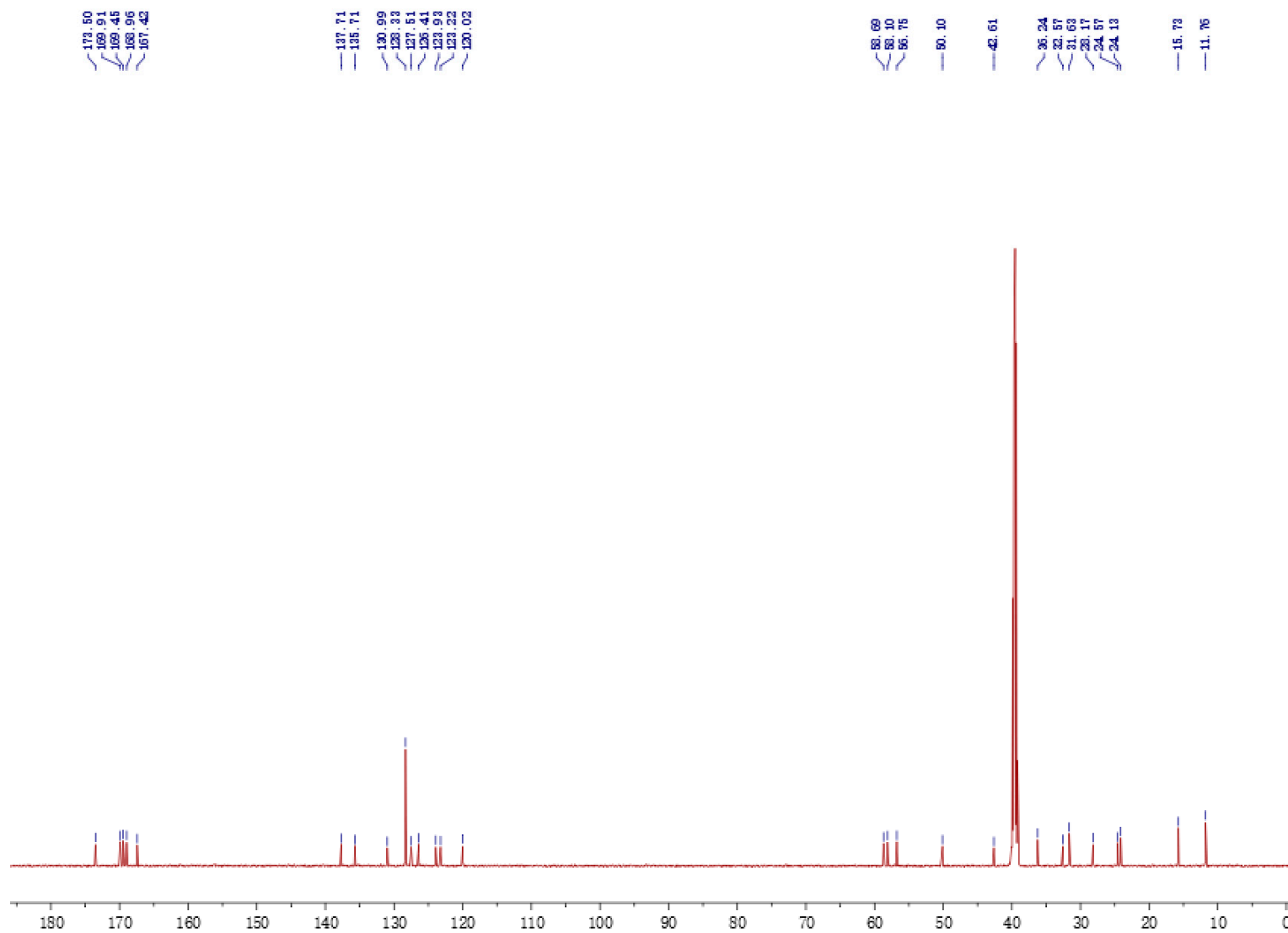


Figure S3. <sup>13</sup>C NMR (DMSO-*d*<sub>6</sub>, 125 MHz) spectrum of **1**.

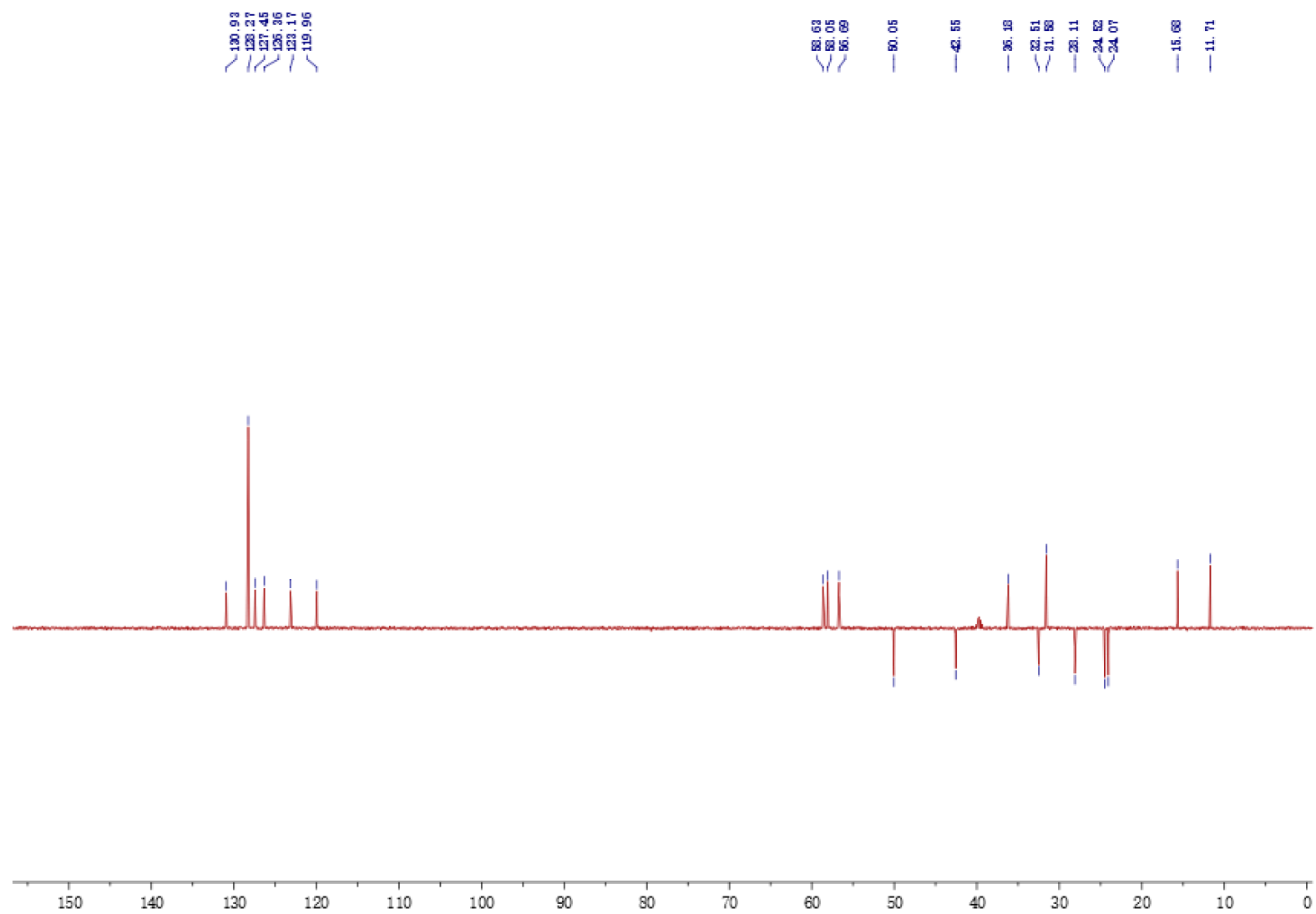


Figure S4. DEPT (DMSO- $d_6$ , 125 MHz) spectrum of **1**.

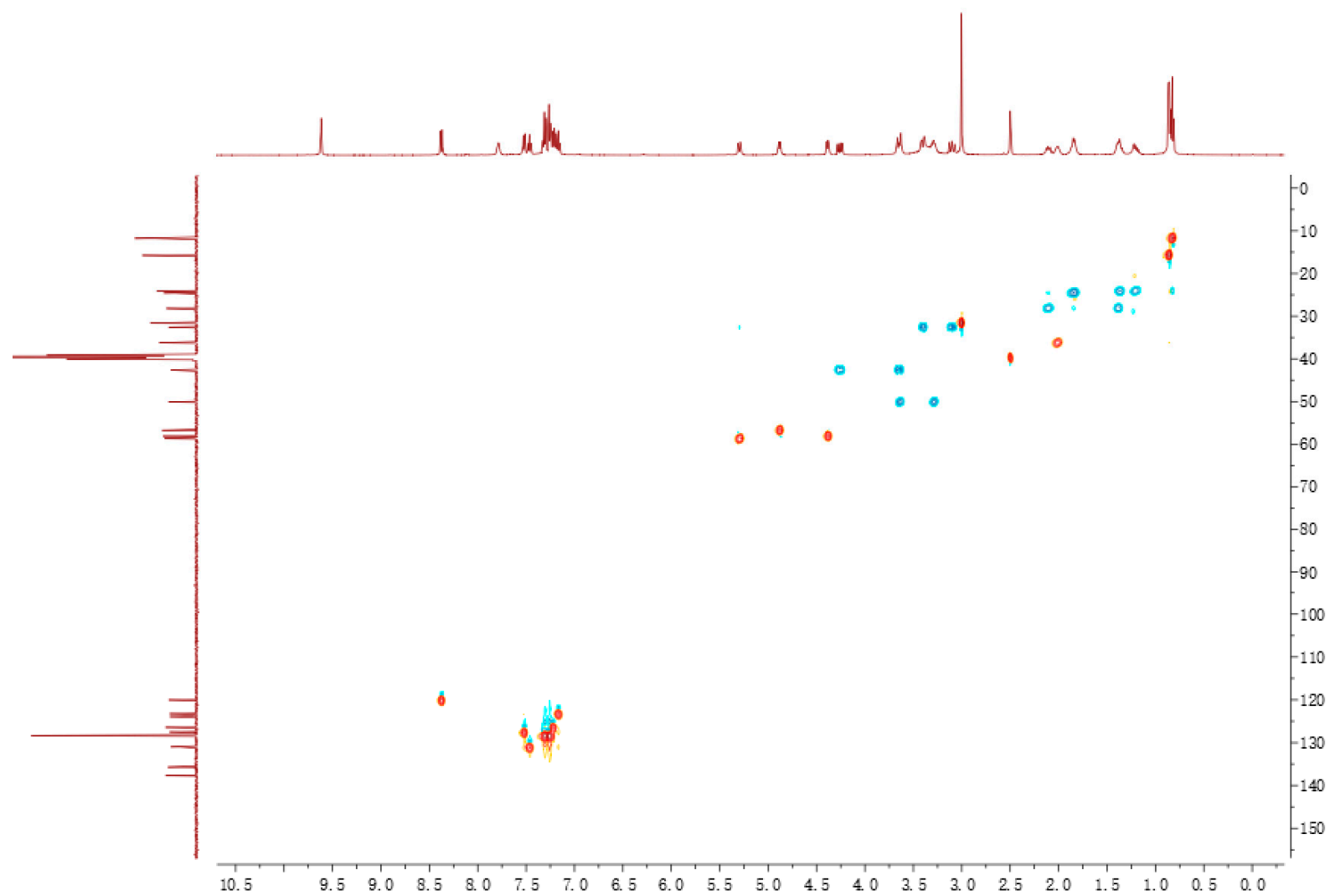


Figure S5. HMQC spectrum of 1.



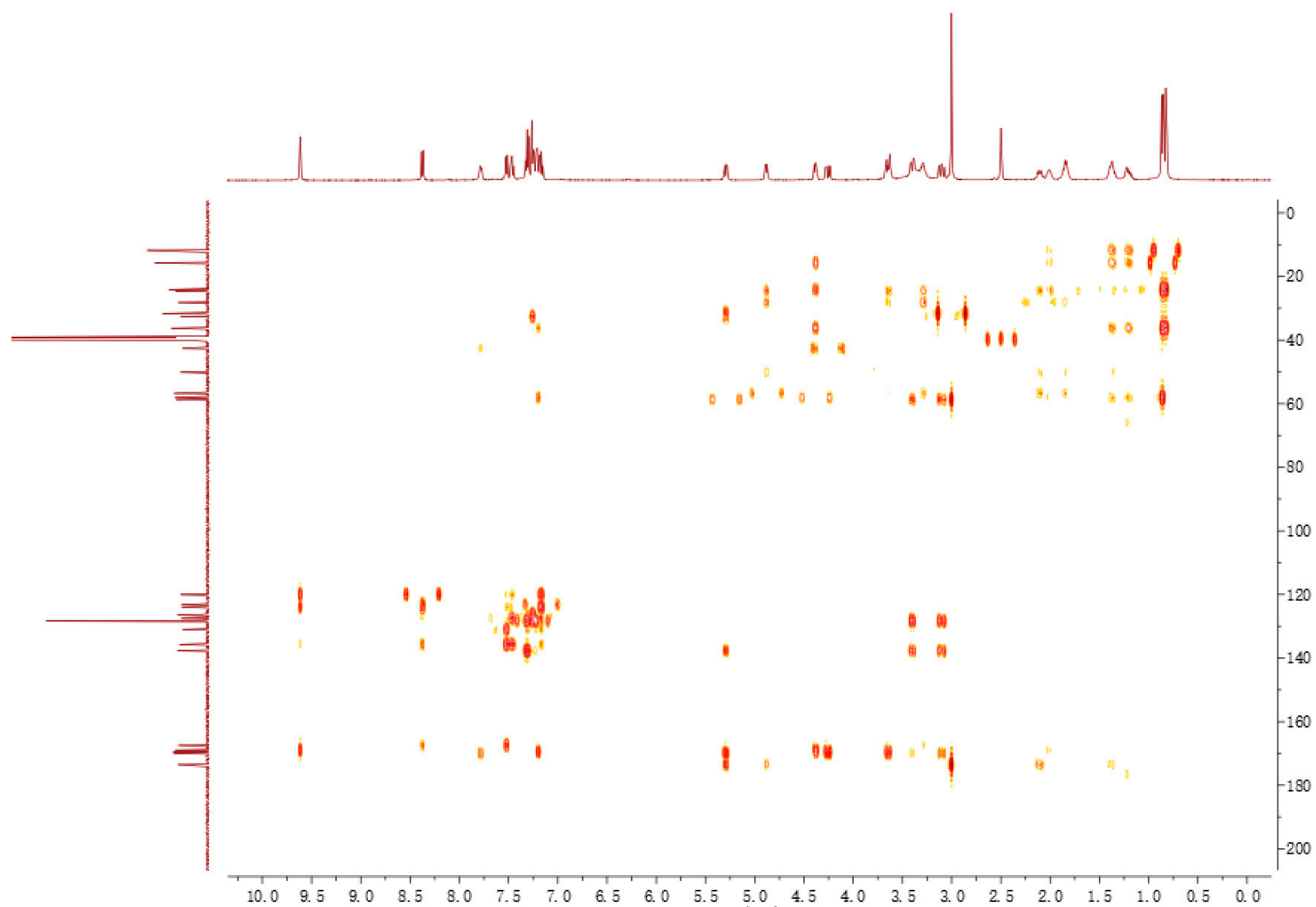


Figure S6. HMBC spectrum of **1**.

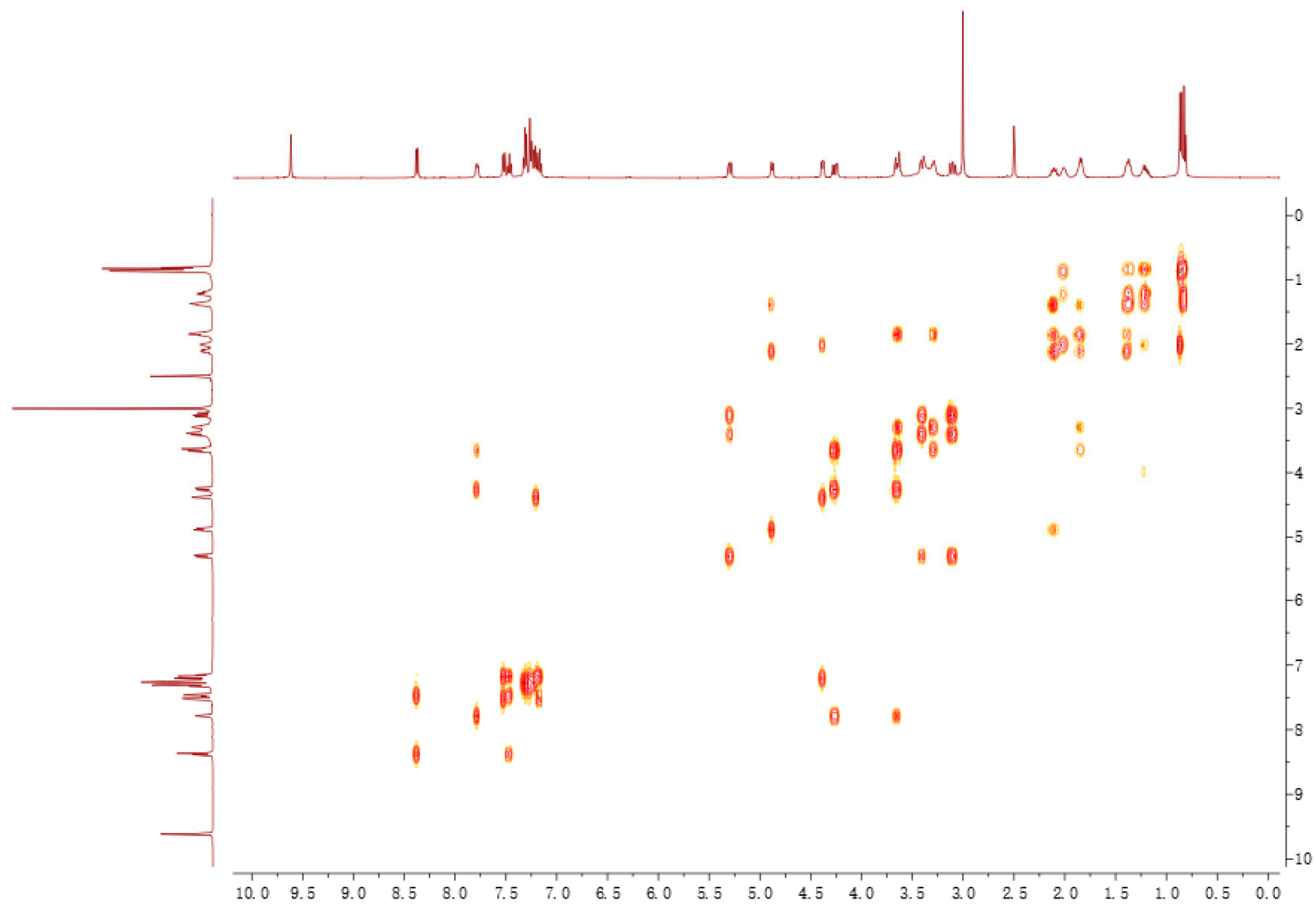


Figure S7.  $^1\text{H}$ - $^1\text{H}$  COSY spectrum of **1**.

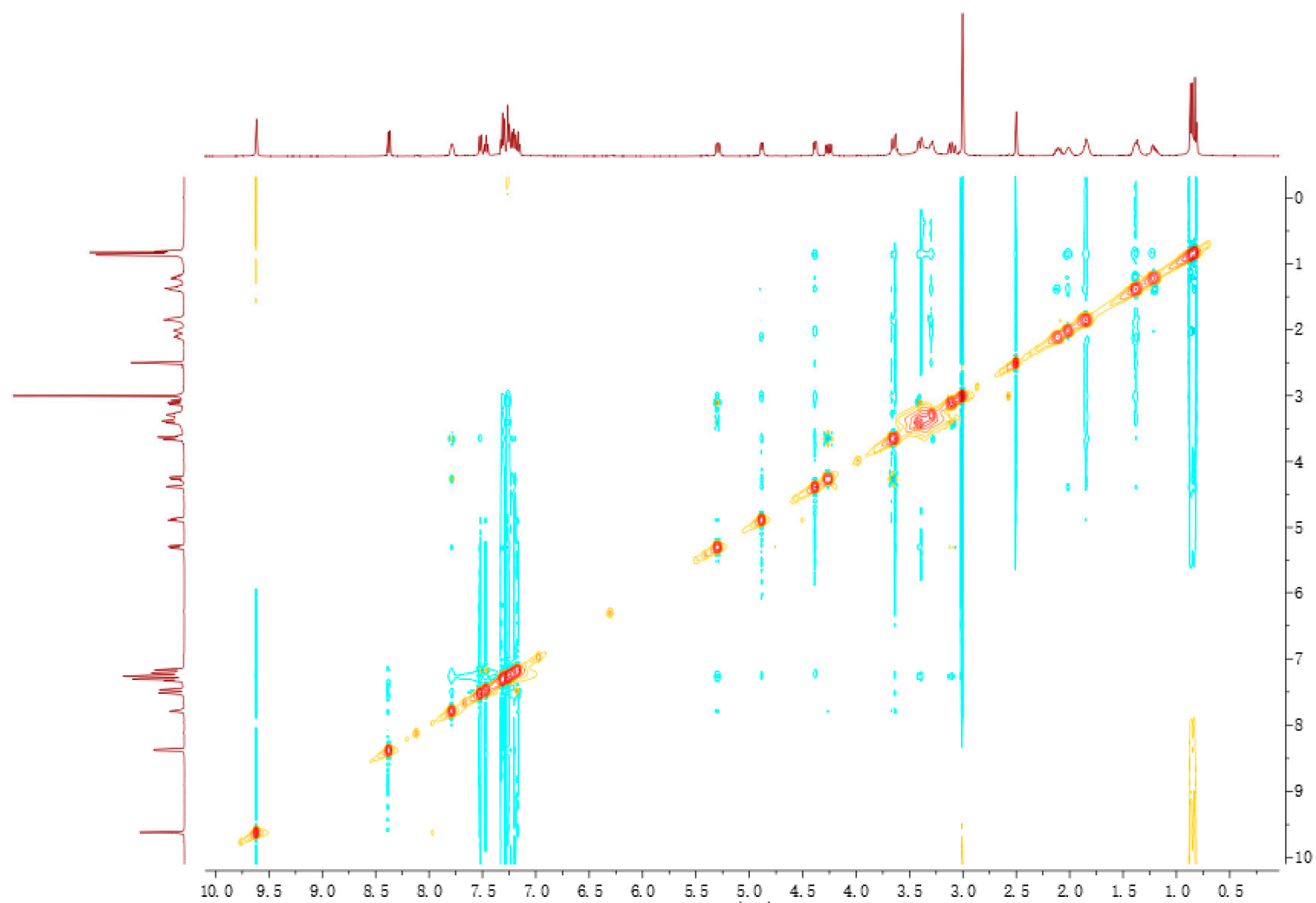


Figure S8. NOESY spectrum of **1**.

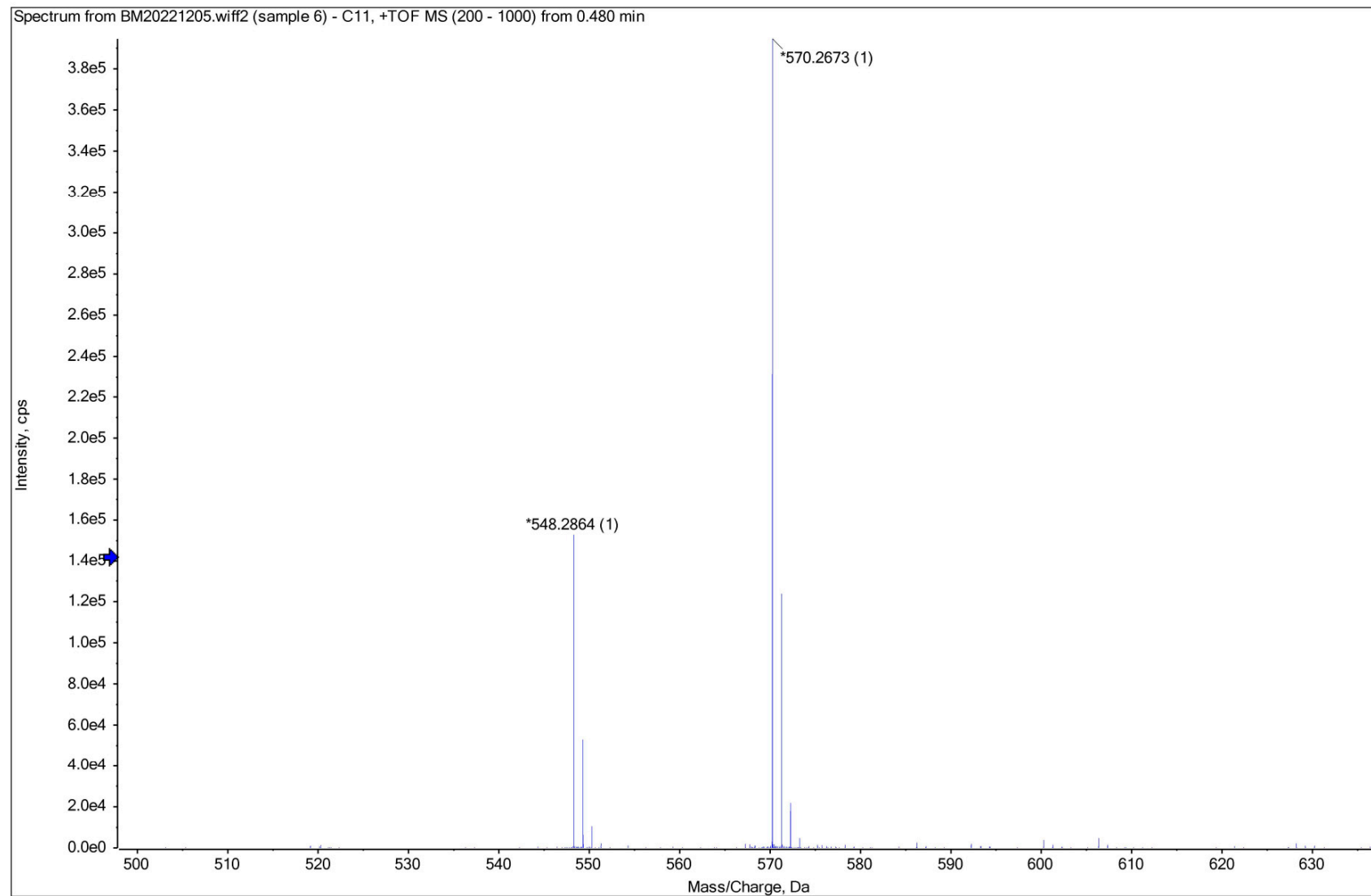


Figure S9. HR-ESI-MS spectrum of **1**.

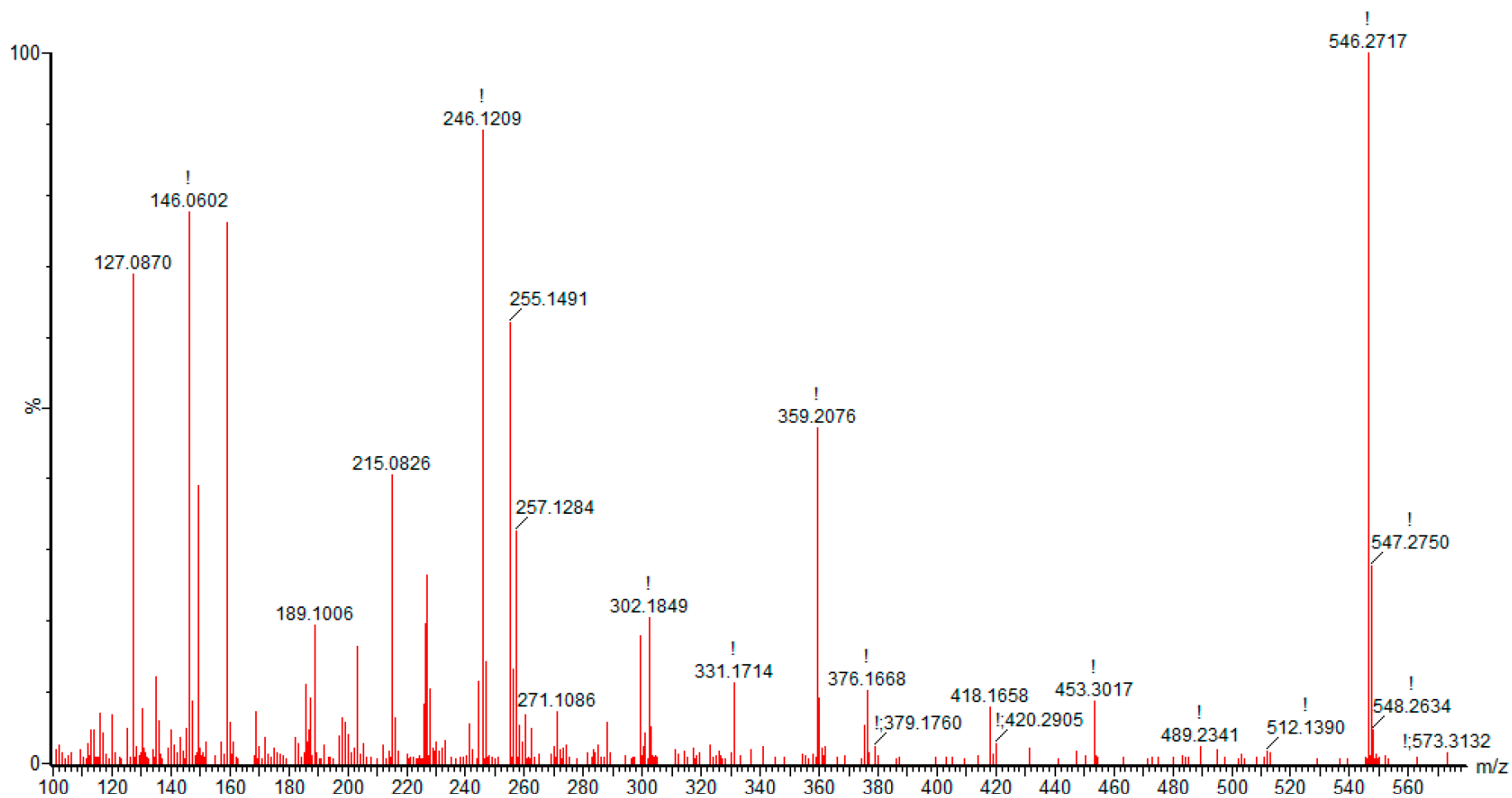


Figure S10. ESI-MS/MS spectrum of **1**

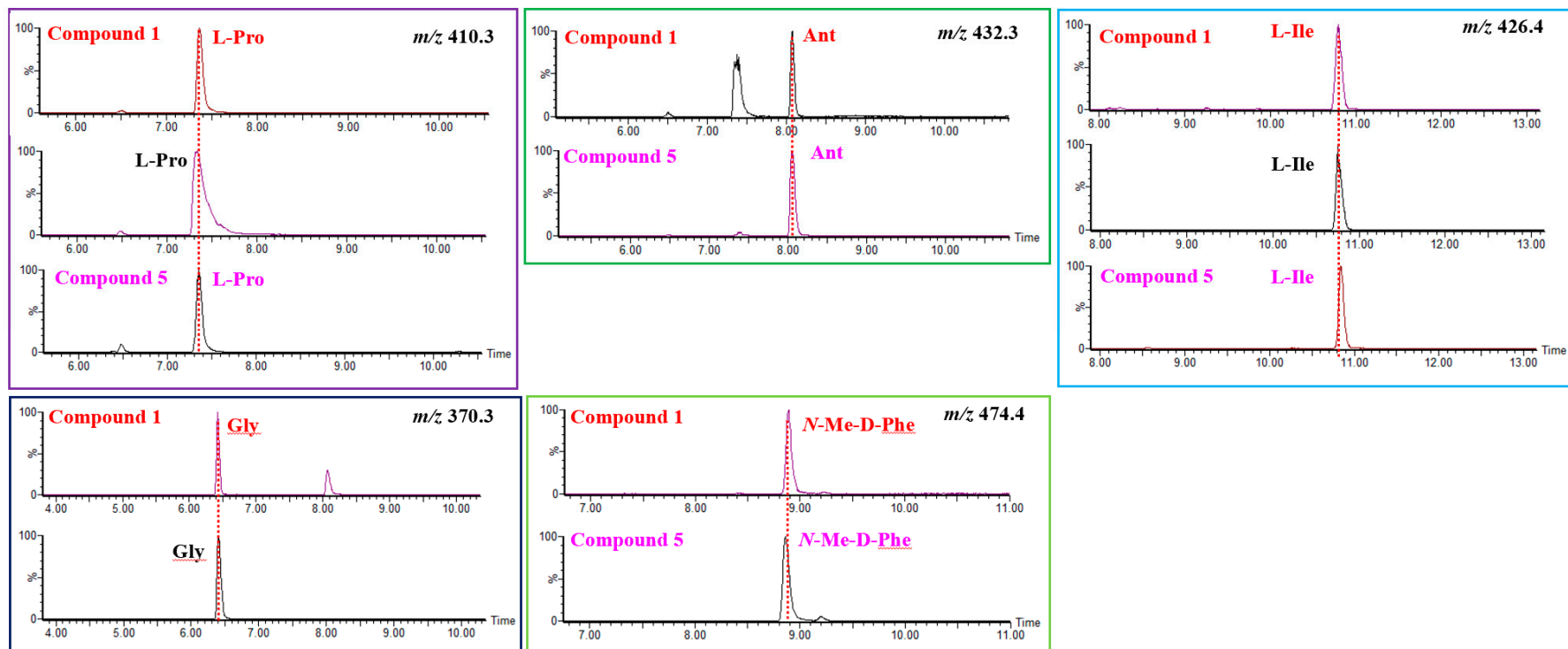


Figure S11. Marfey's analysis of **1**.

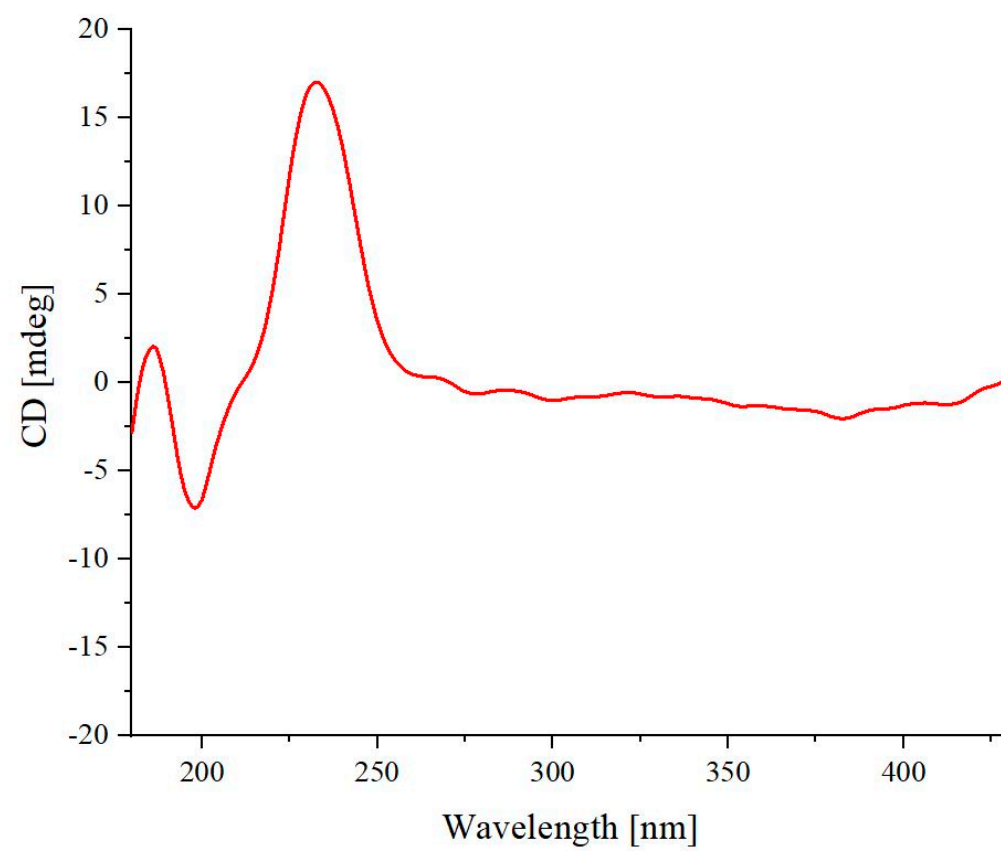


Figure S12. CD spectrum of **1** in MeOH.

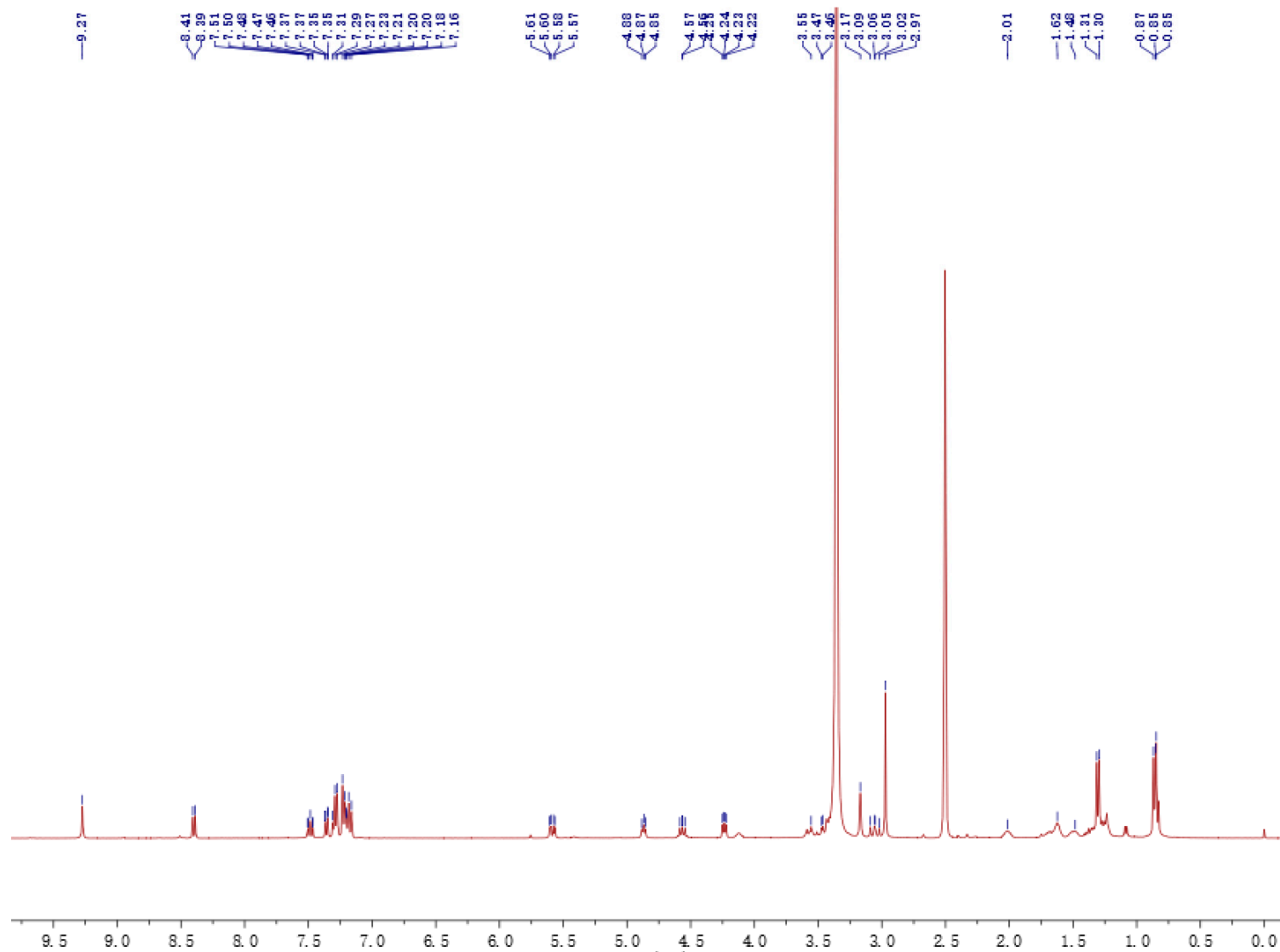


Figure S13.  $^1\text{H}$  NMR ( $\text{DMSO-}d_6$ , 400 MHz) spectrum of **2**.



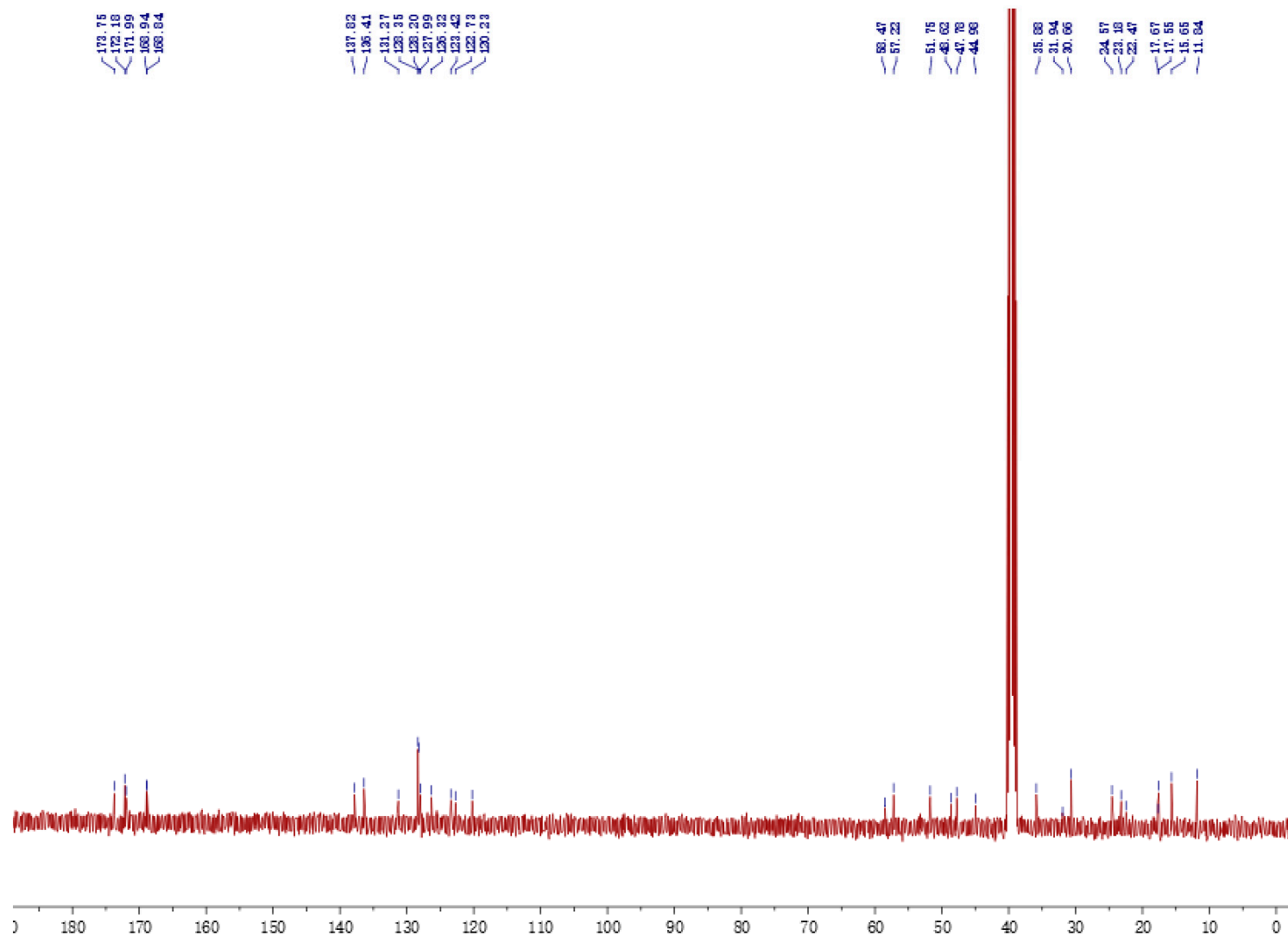


Figure S14.  $^{13}\text{C}$  NMR ( $\text{DMSO}-d_6$ , 100MHz) spectrum of **2**.

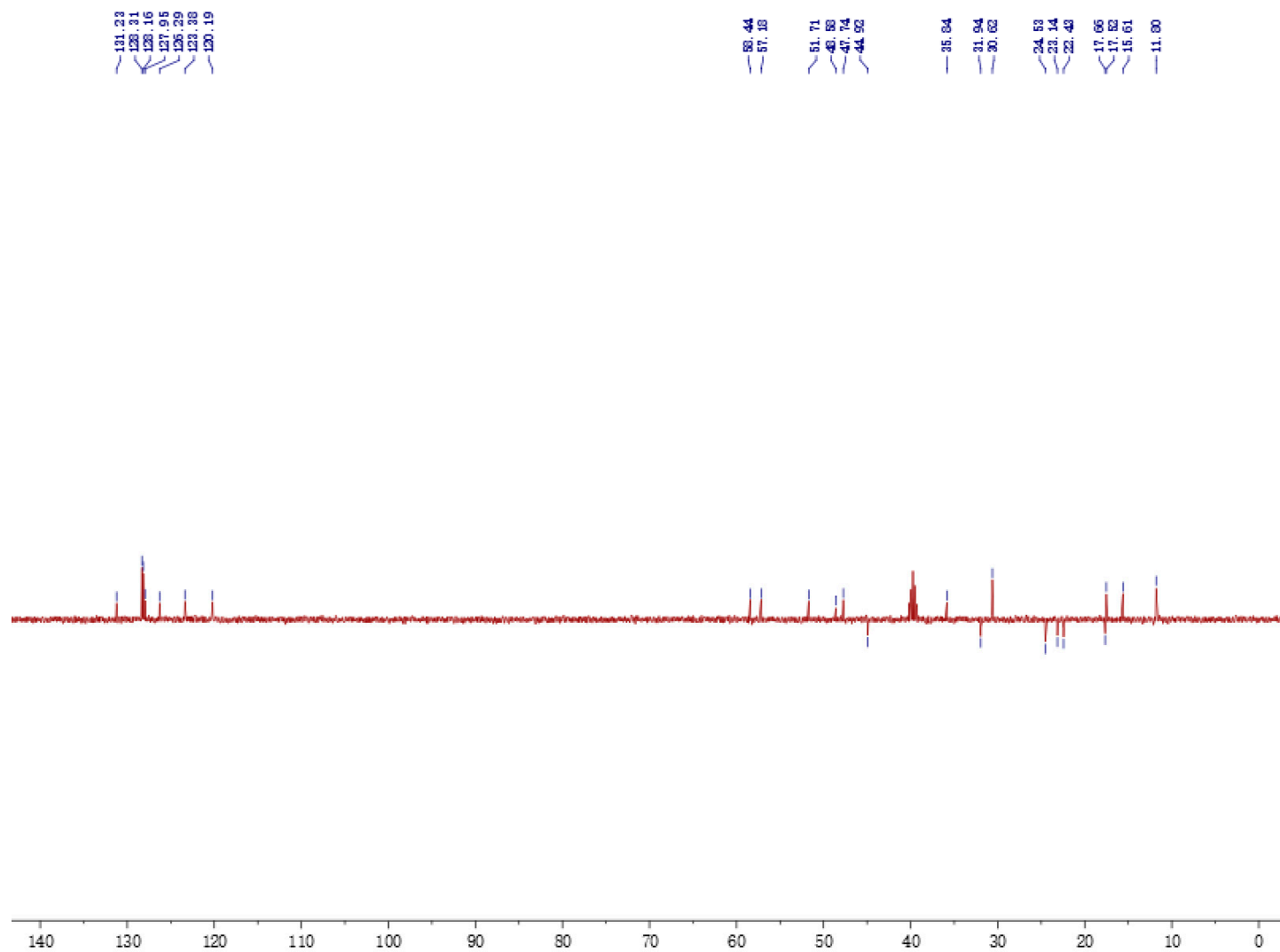


Figure S15. DEPT (DMSO- $d_6$ , 100 MHz) spectrum of **2**.

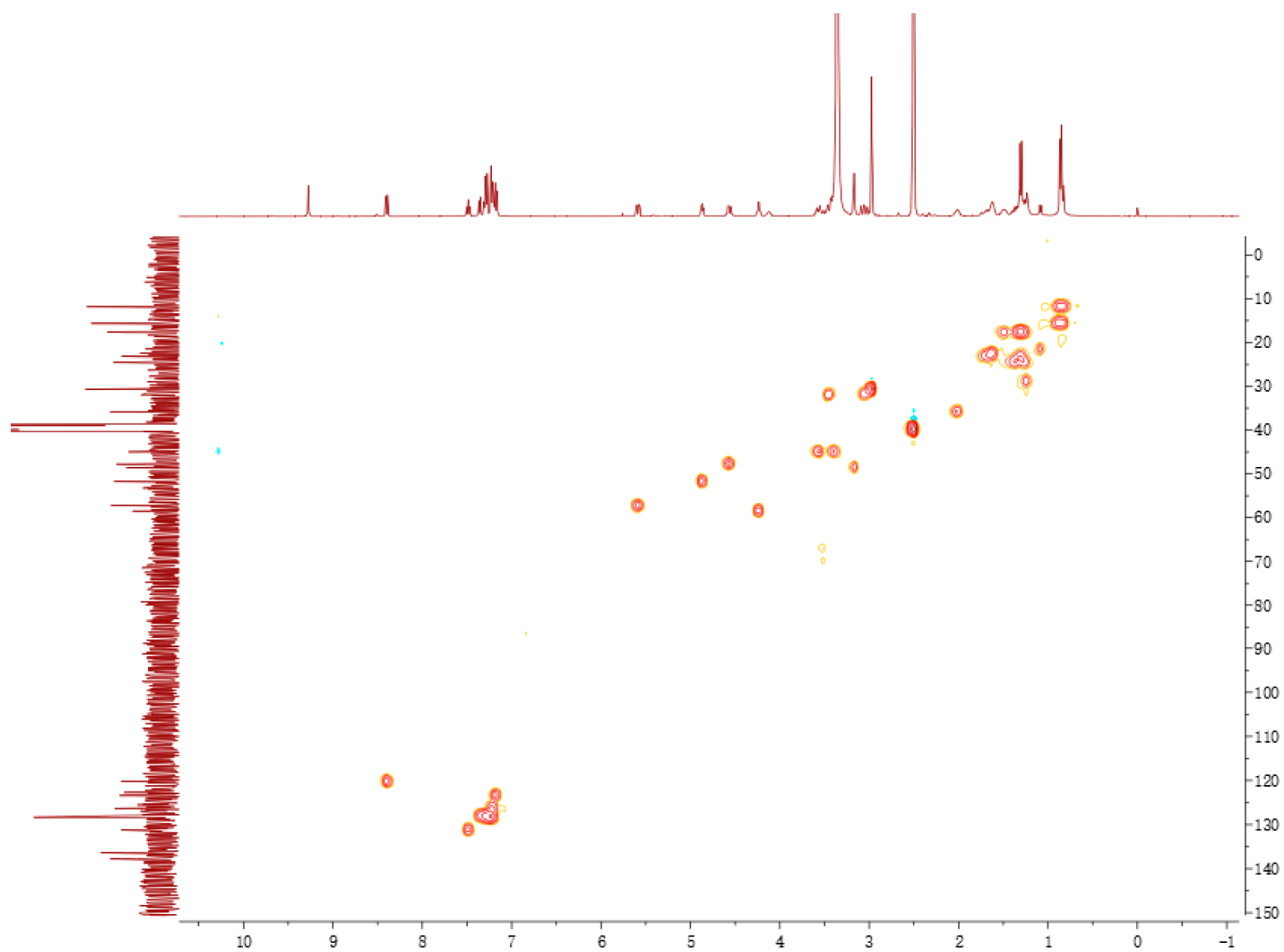


Figure S16. HMQC spectrum of **2**.

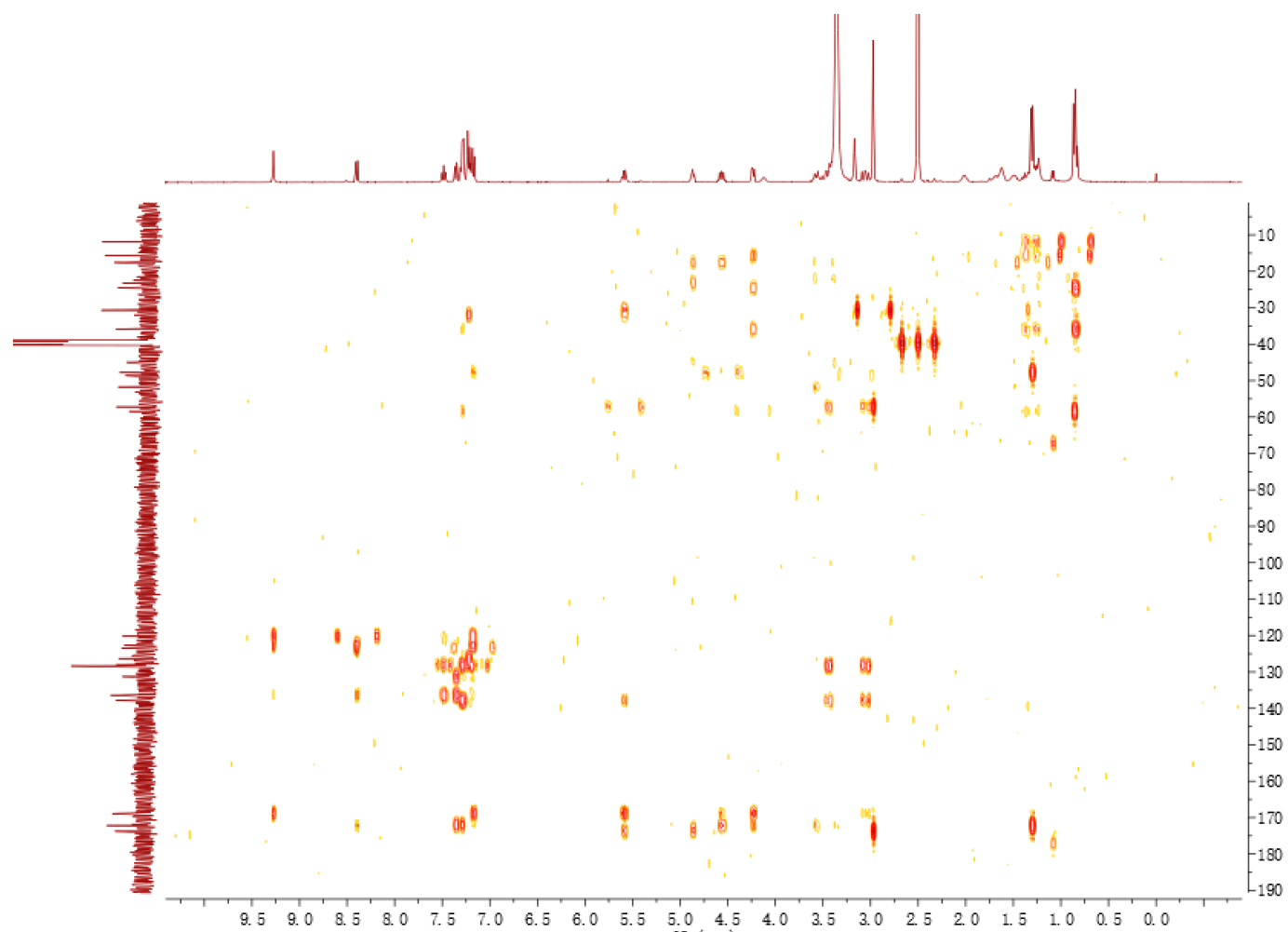


Figure S17. HMBC spectrum of **2**.

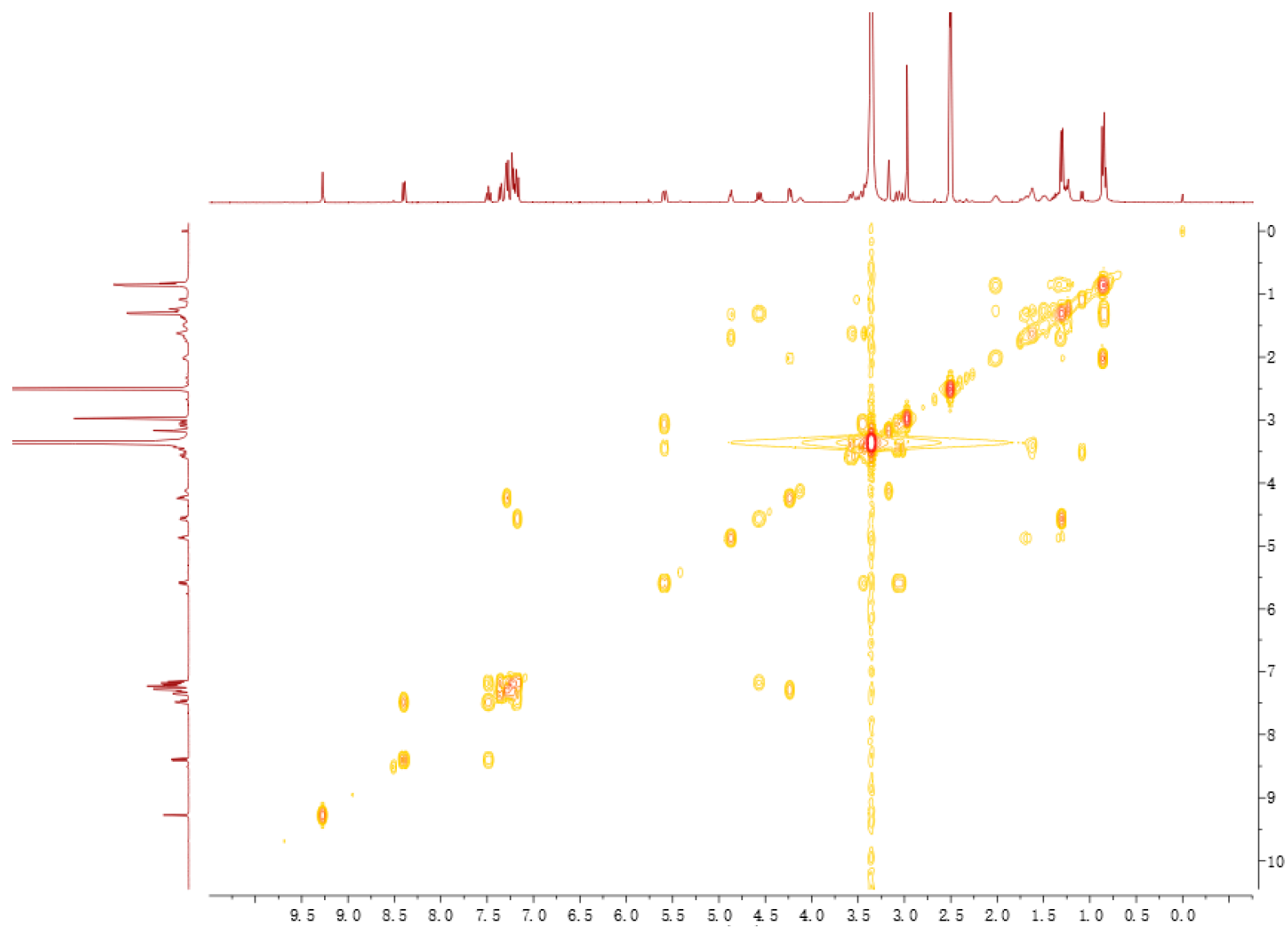


Figure S18.  $^1\text{H}$ - $^1\text{H}$  COSY spectrum of **2**.

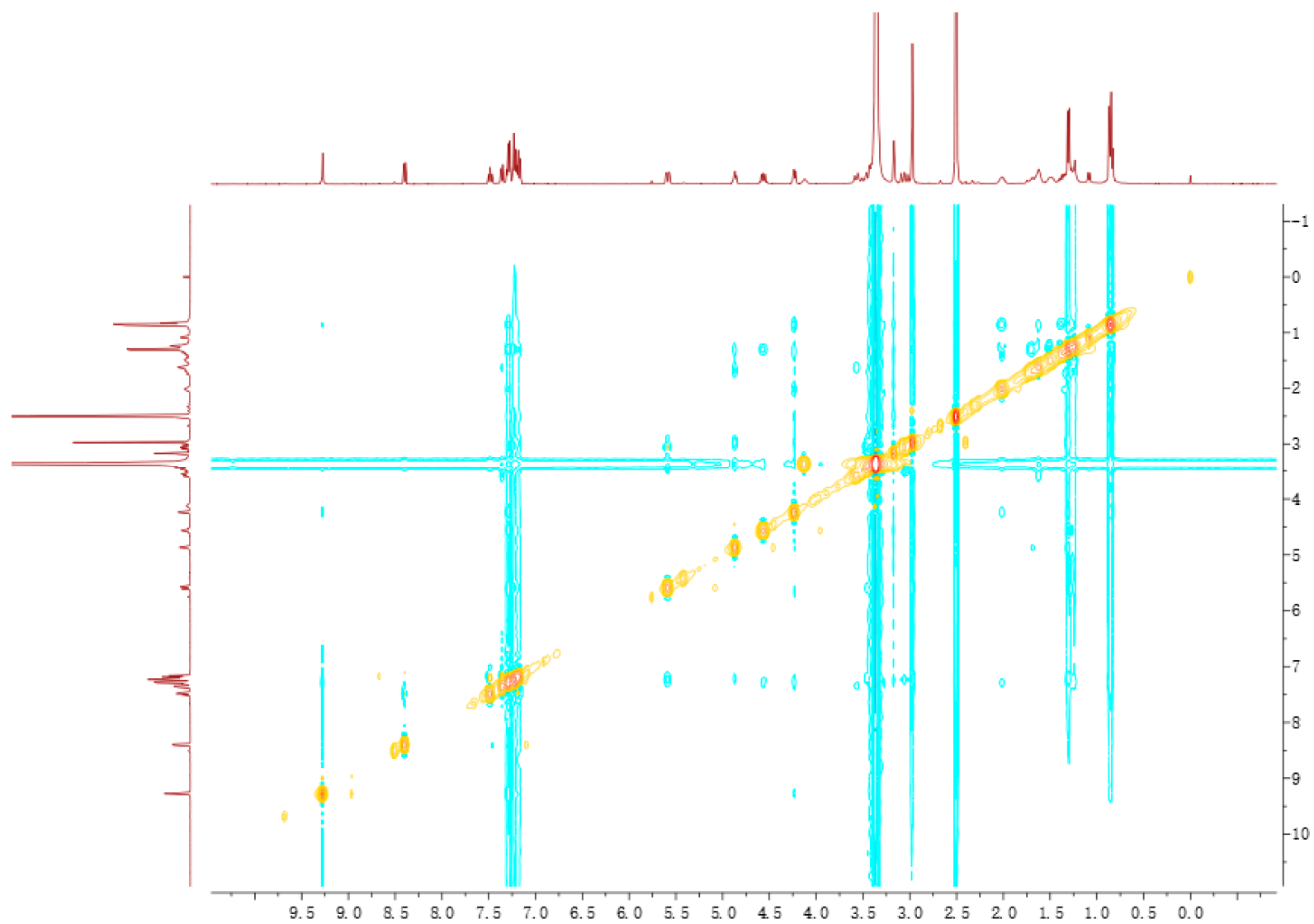


Figure S19. NOESY spectrum of 2.

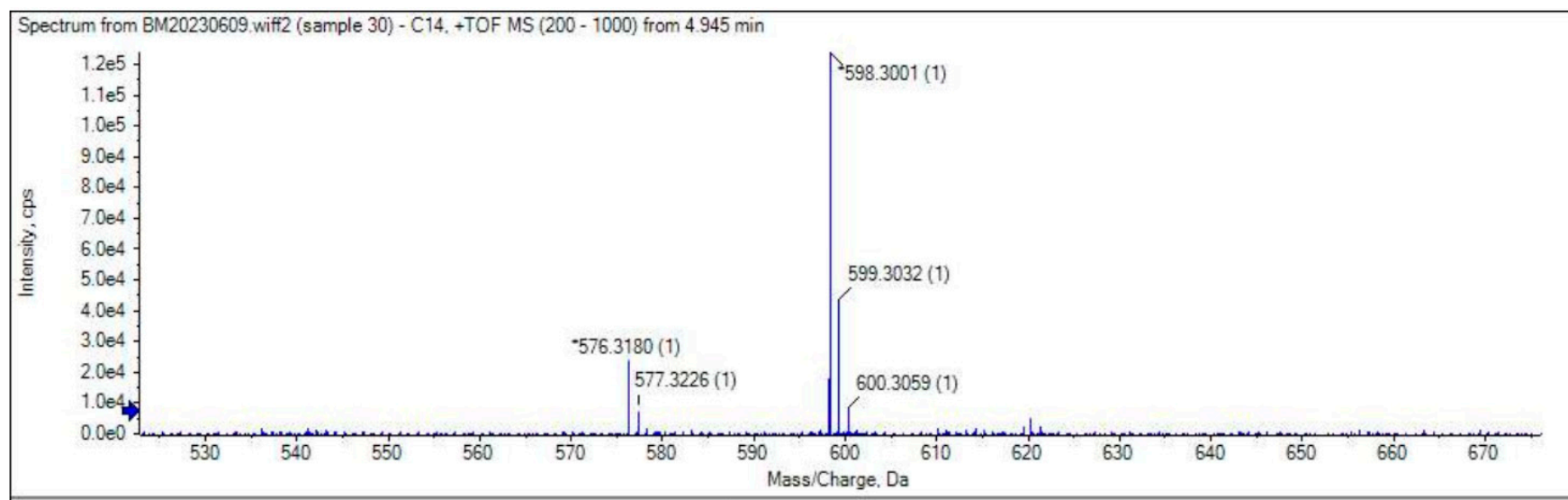


Figure S20. HR-ESI-MS spectrum of **2**.

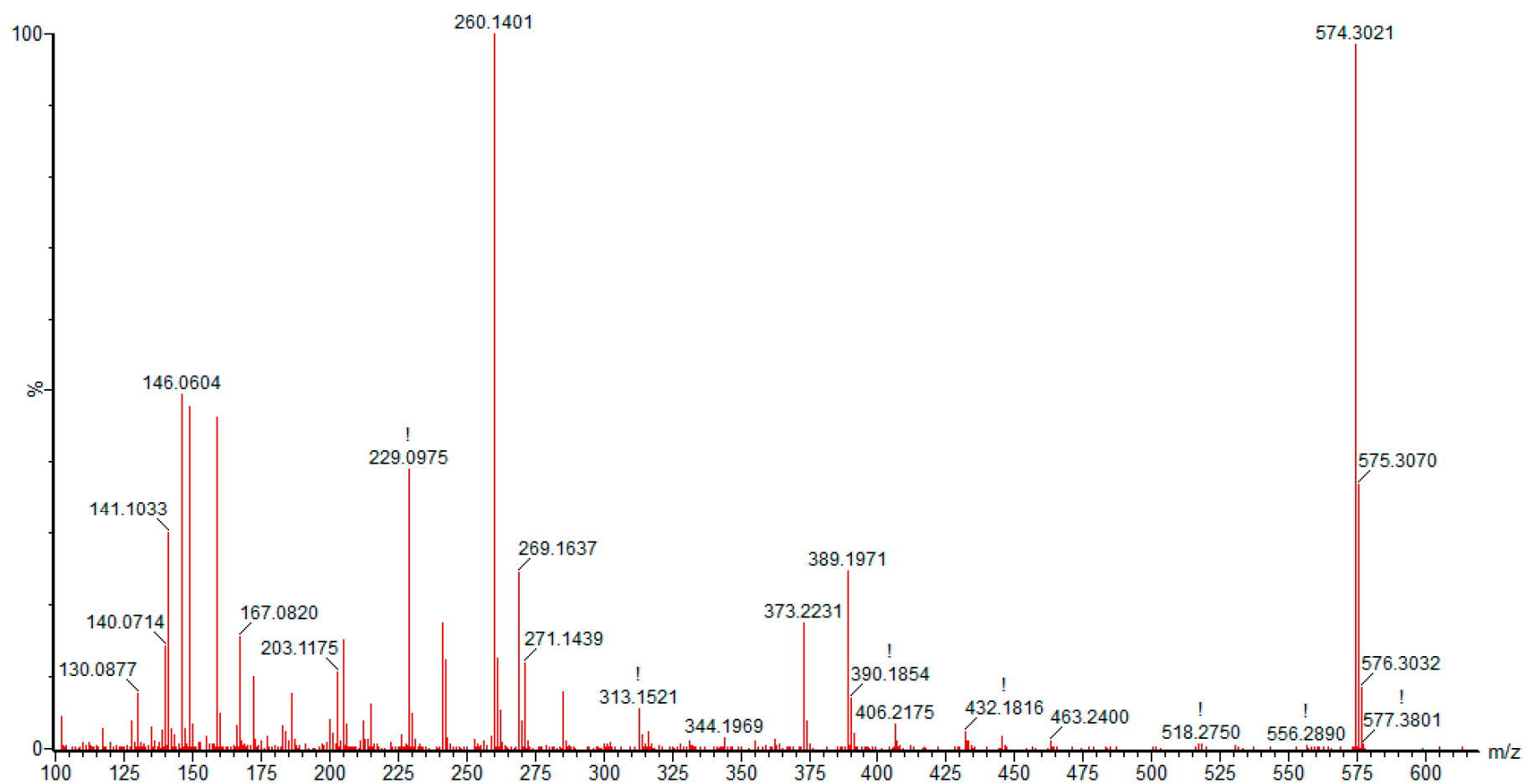


Figure S21. ESI-MS/MS spectrum of 2.



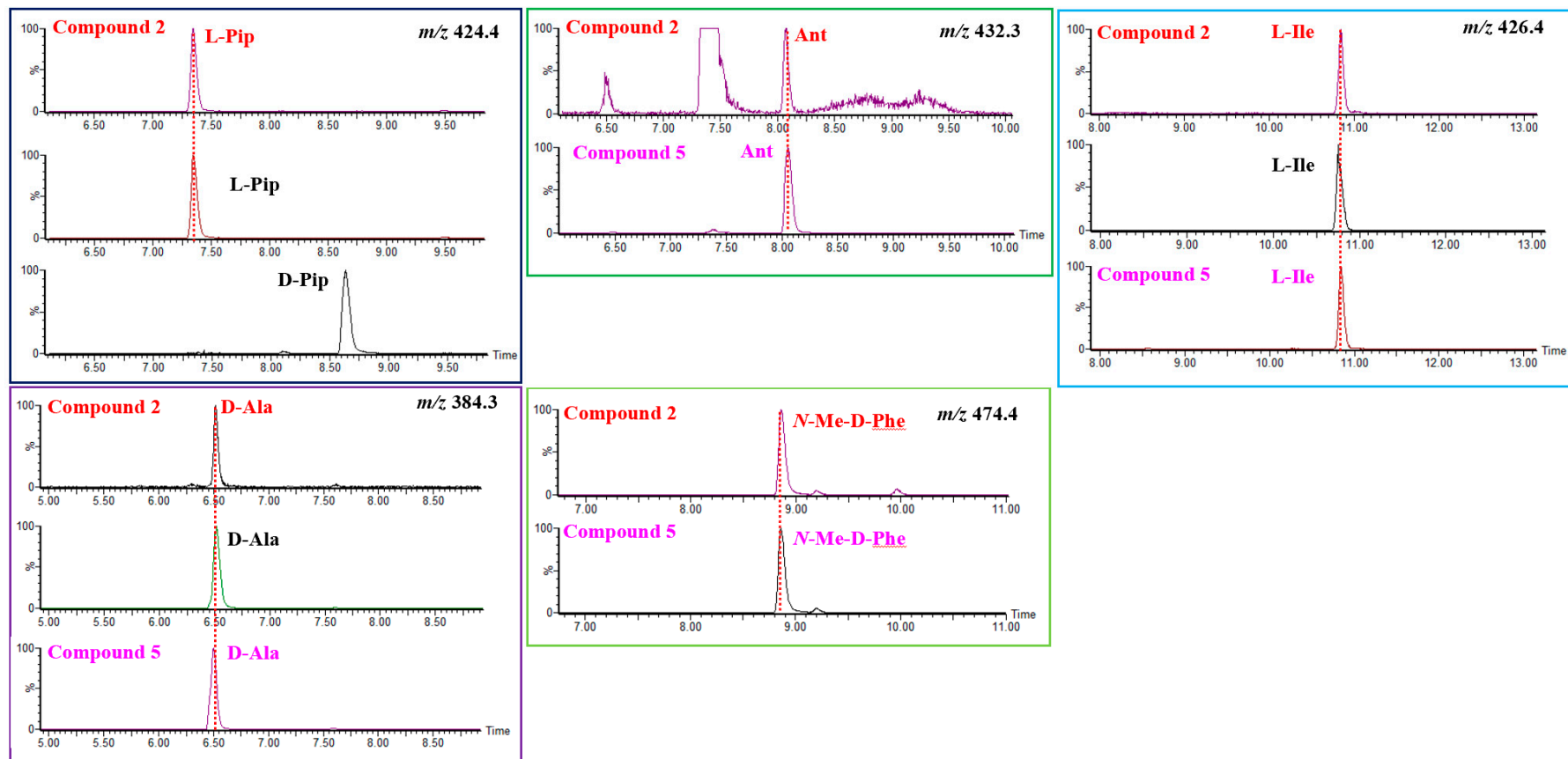


Figure S22. Marfey's analysis of 2.

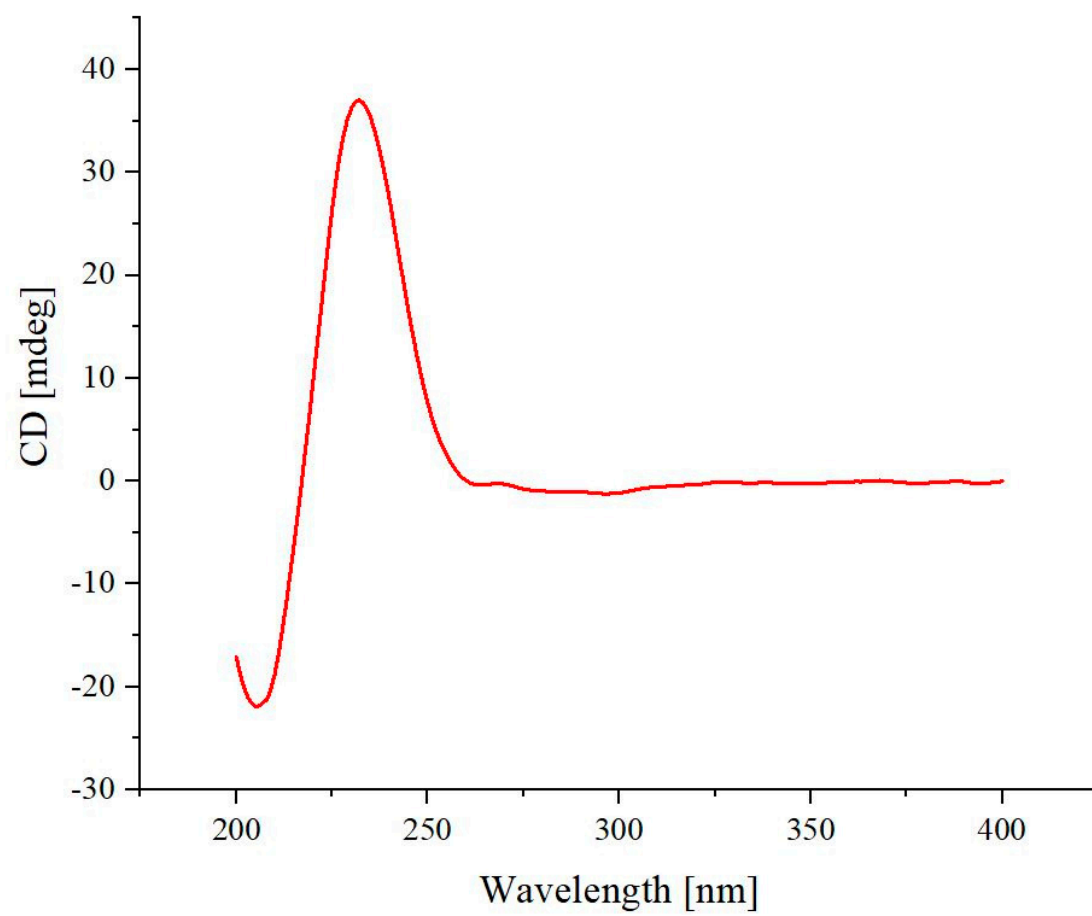


Figure S23. CD spectrum of **2** in MeOH.

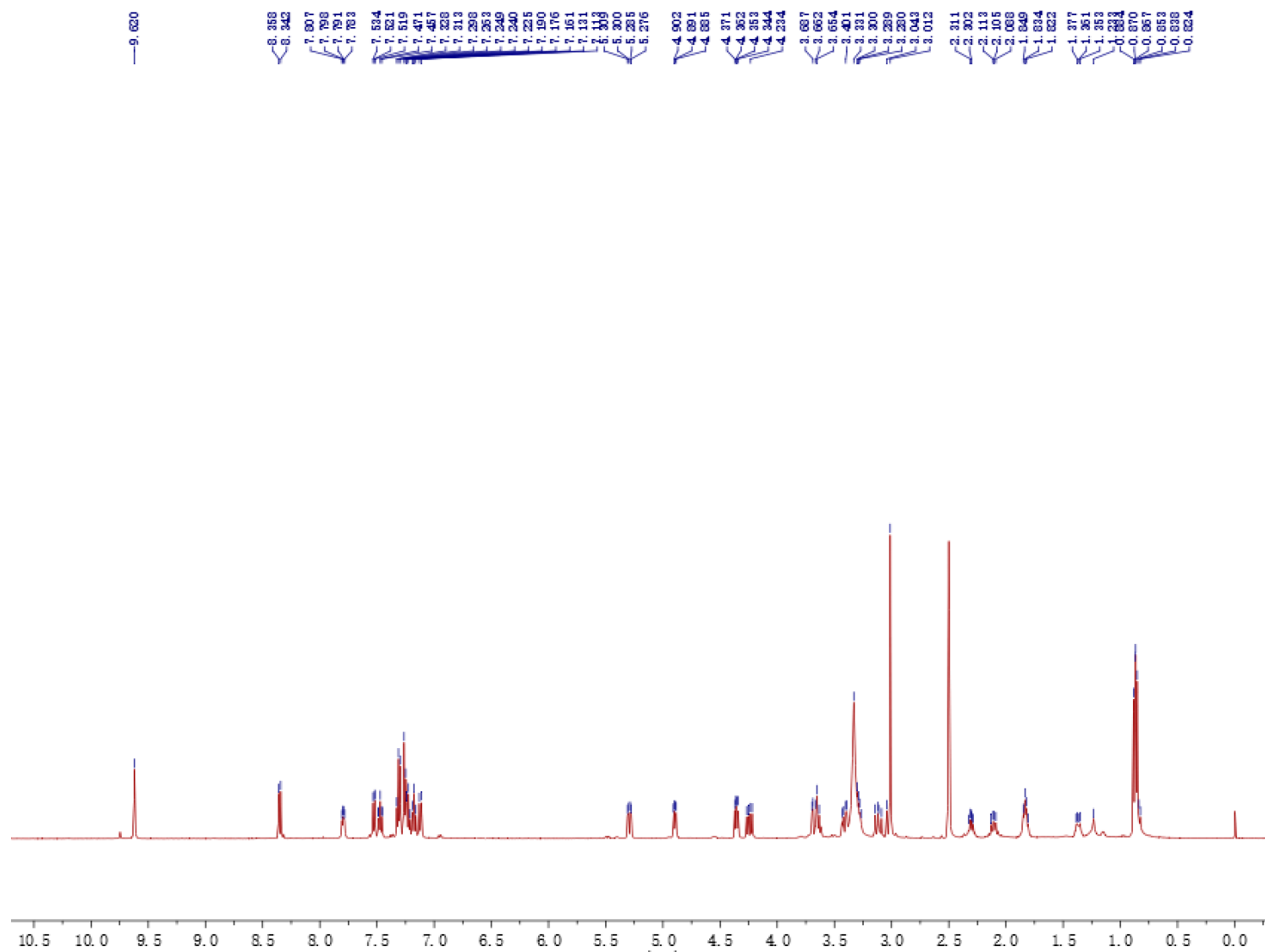


Figure S24.  $^1\text{H}$  NMR ( $\text{DMSO-}d_6$ , 500 MHz) spectrum of **3**.

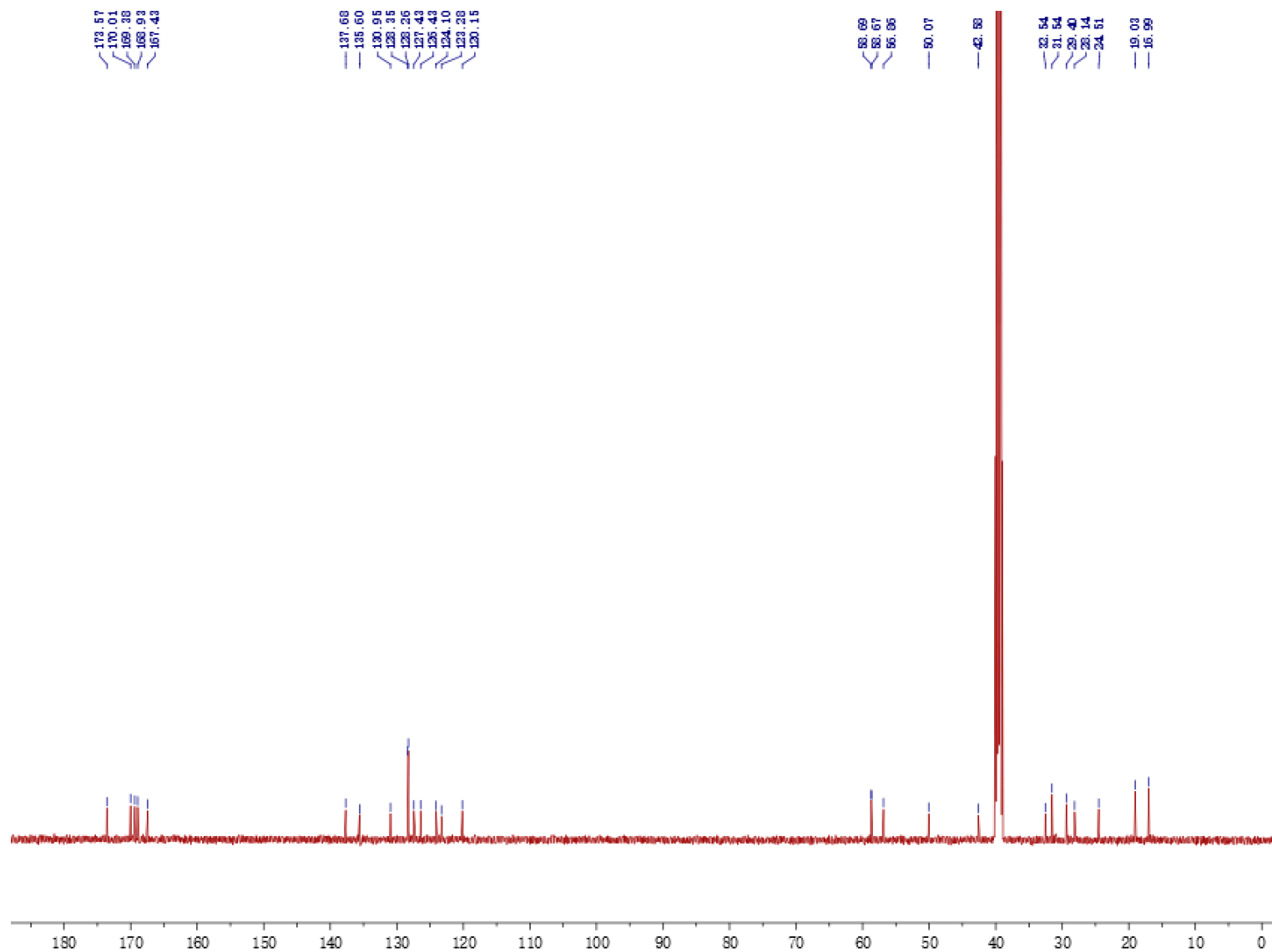


Figure S25. <sup>13</sup>C NMR (DMSO-*d*<sub>6</sub>, 125 MHz) spectrum of 3.

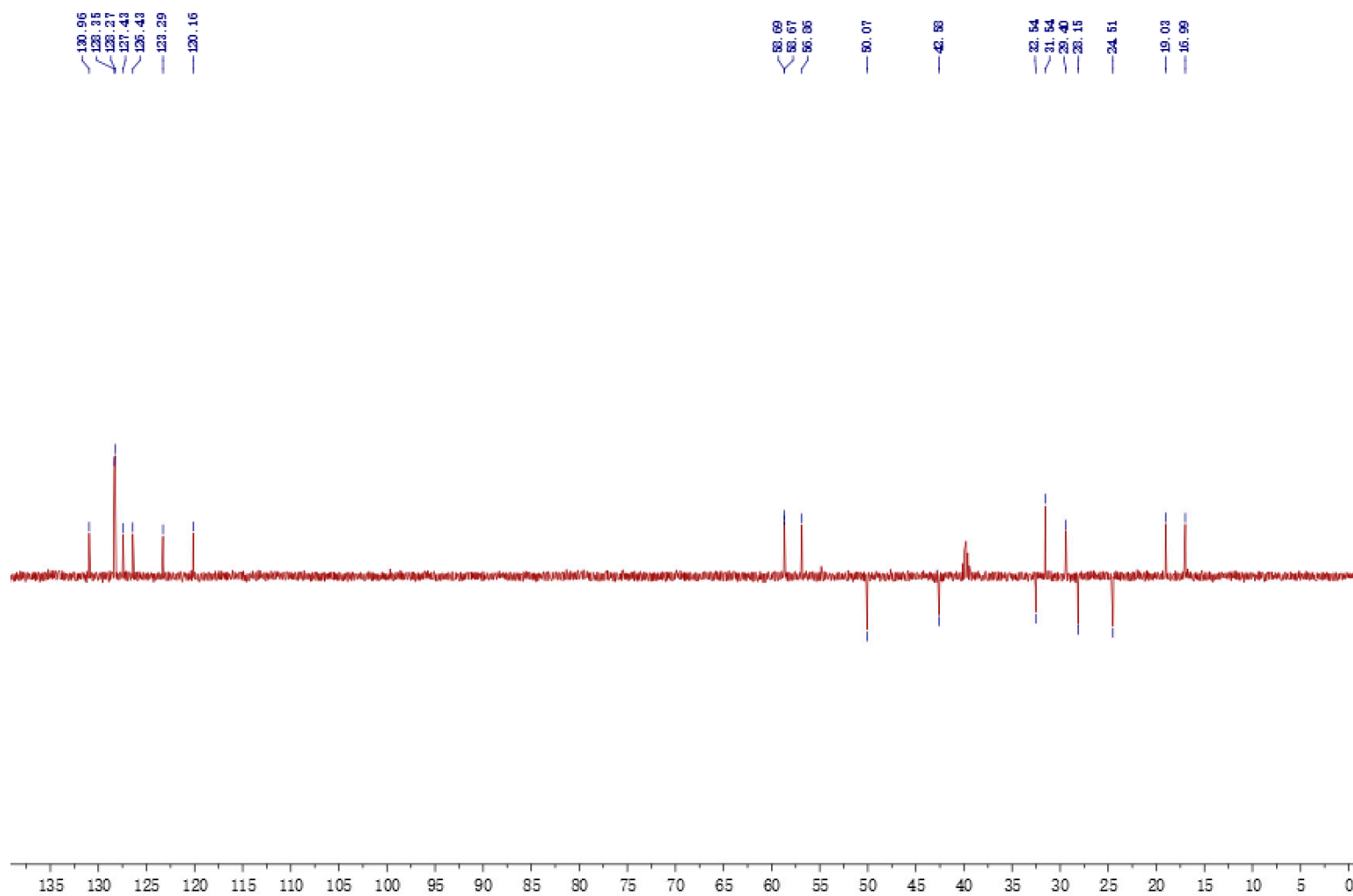


Figure S26. DEPT (DMSO- $d_6$ , 125 MHz) spectrum of **3**.

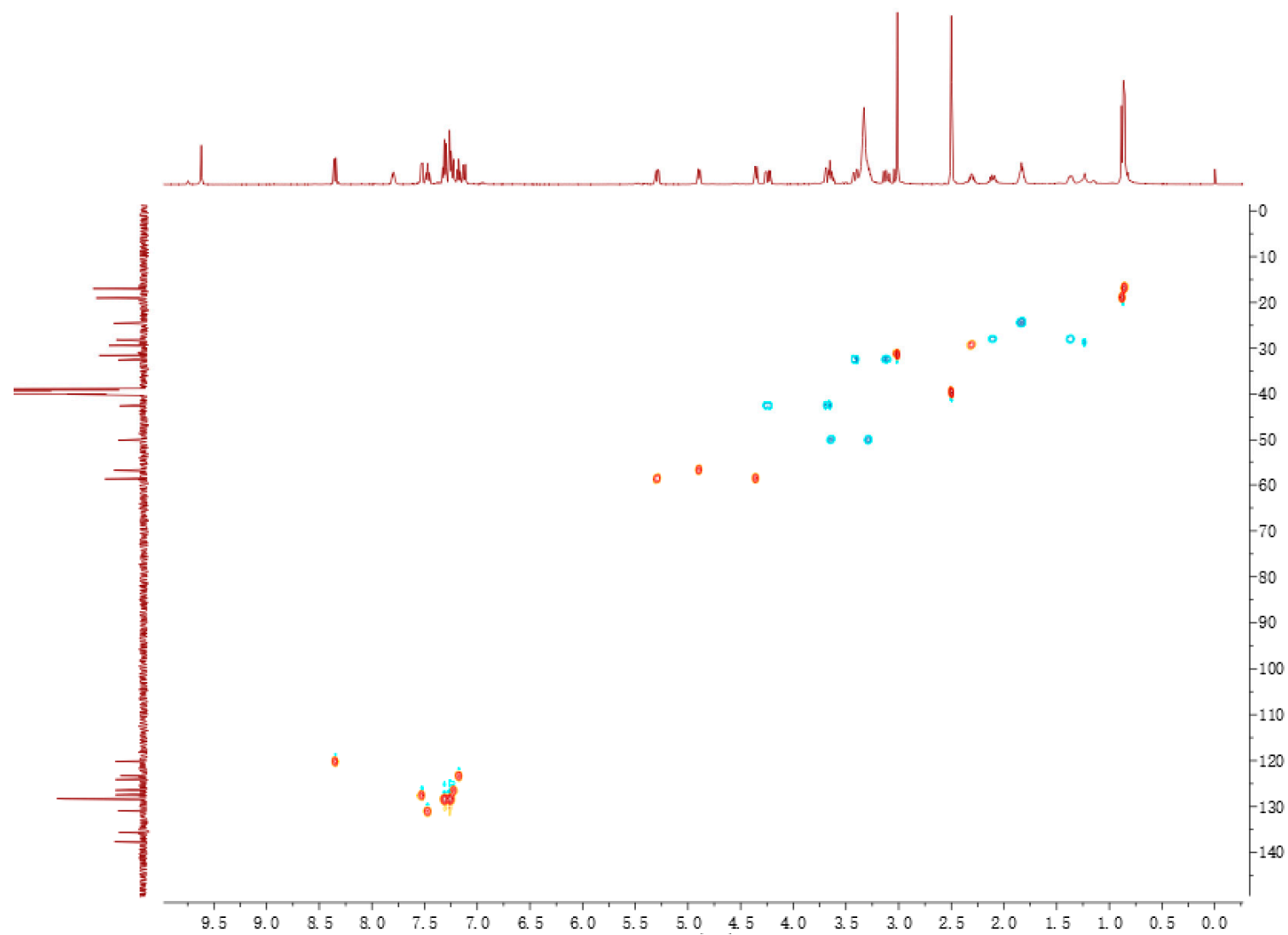


Figure S27. HMQC spectrum of **3**.

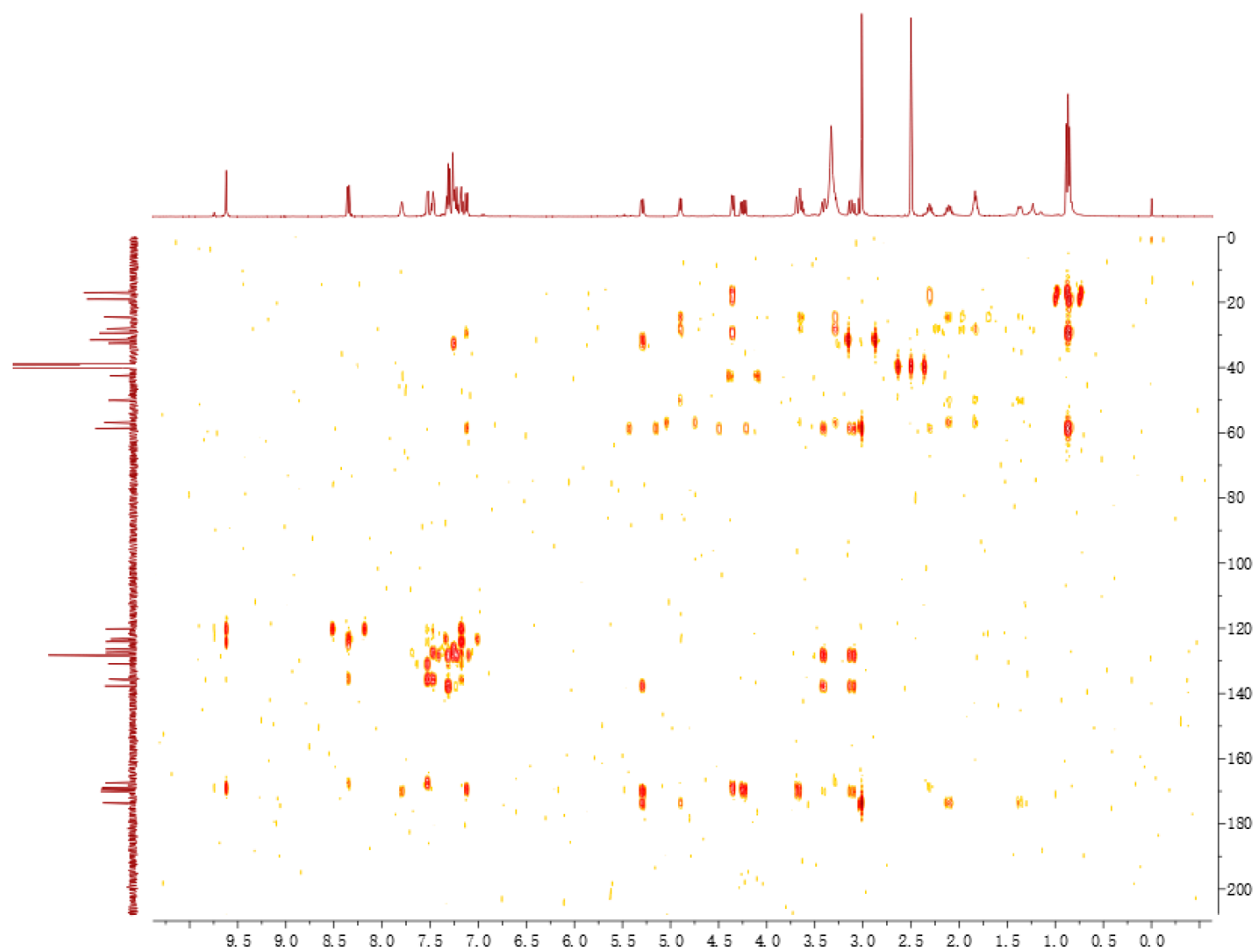


Figure S28. HMBC spectrum of **3**.

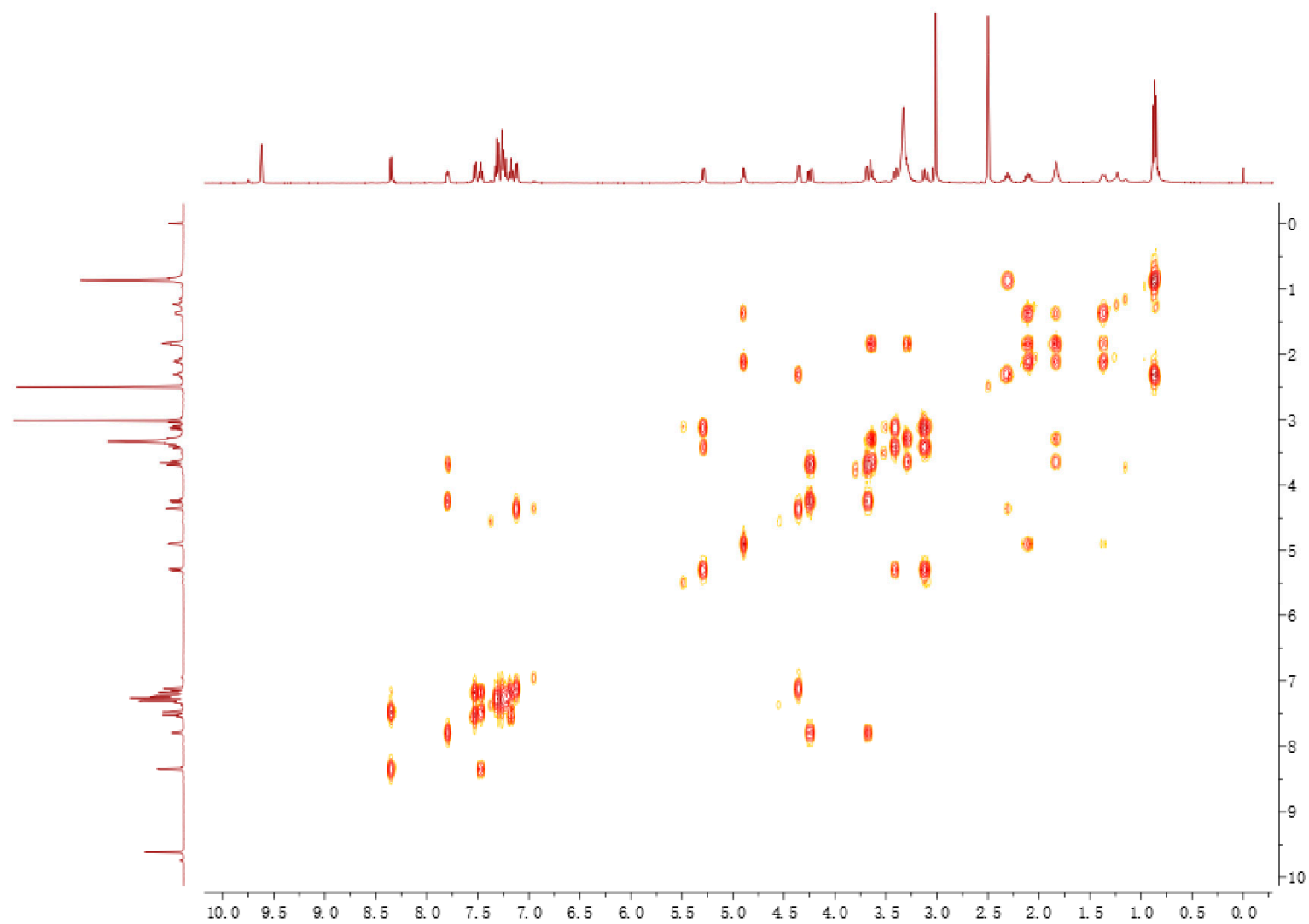


Figure S29.  $^1\text{H}$ - $^1\text{H}$  COSY spectrum of **3**.



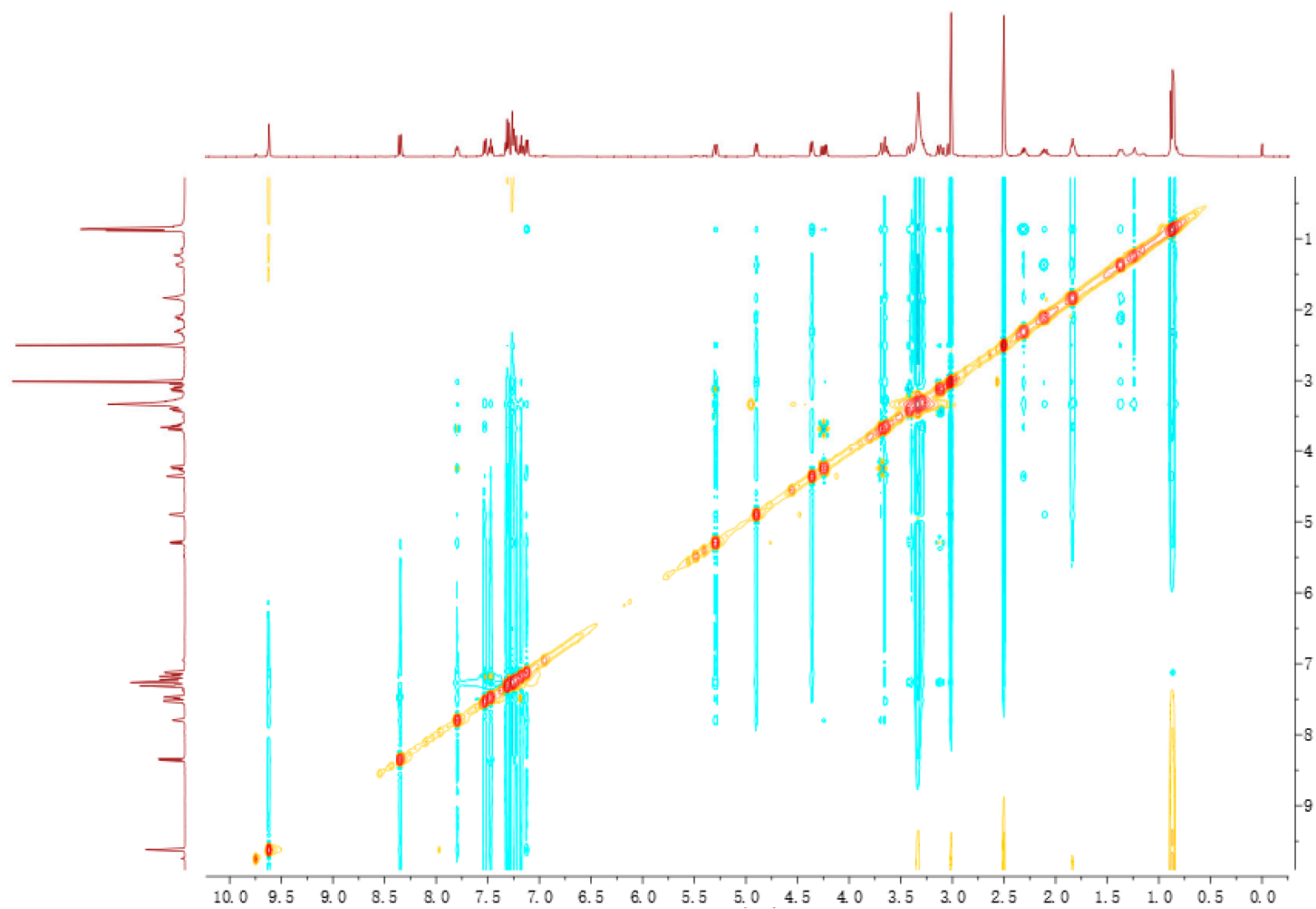


Figure S30. NOESY spectrum of 3.

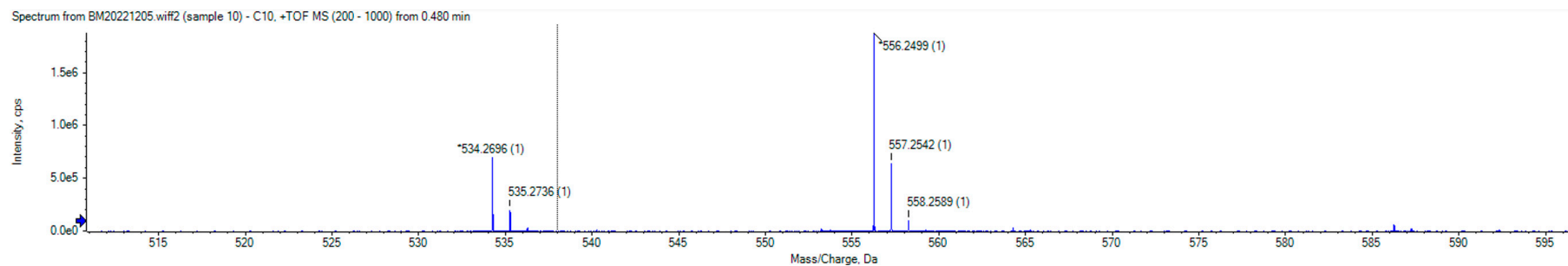


Figure S31. HR-ESI-MS spectrum of **3**.

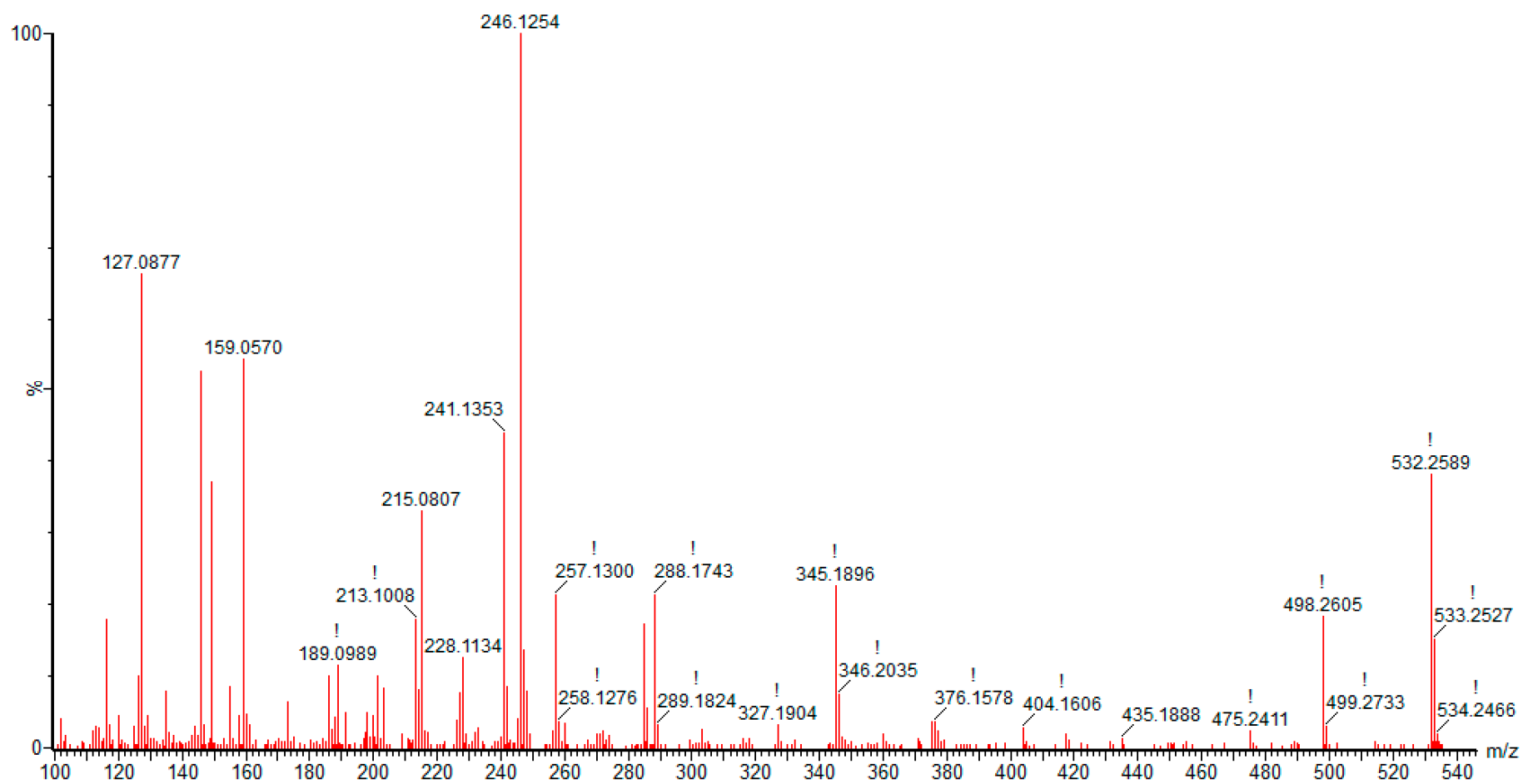


Figure S32. ESI-MS/MS spectrum of 3.

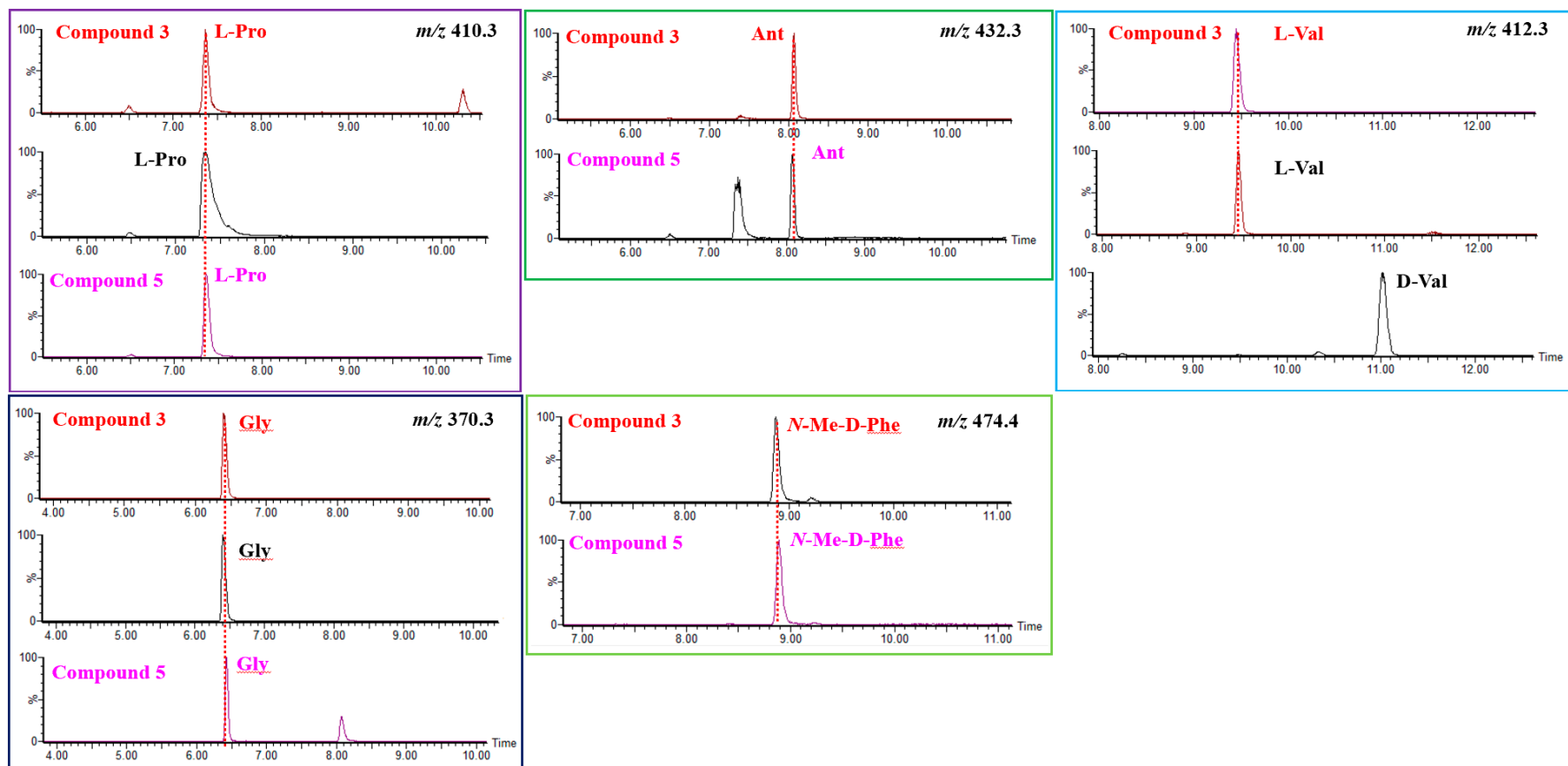


Figure S33. Marfey's analysis of 3.

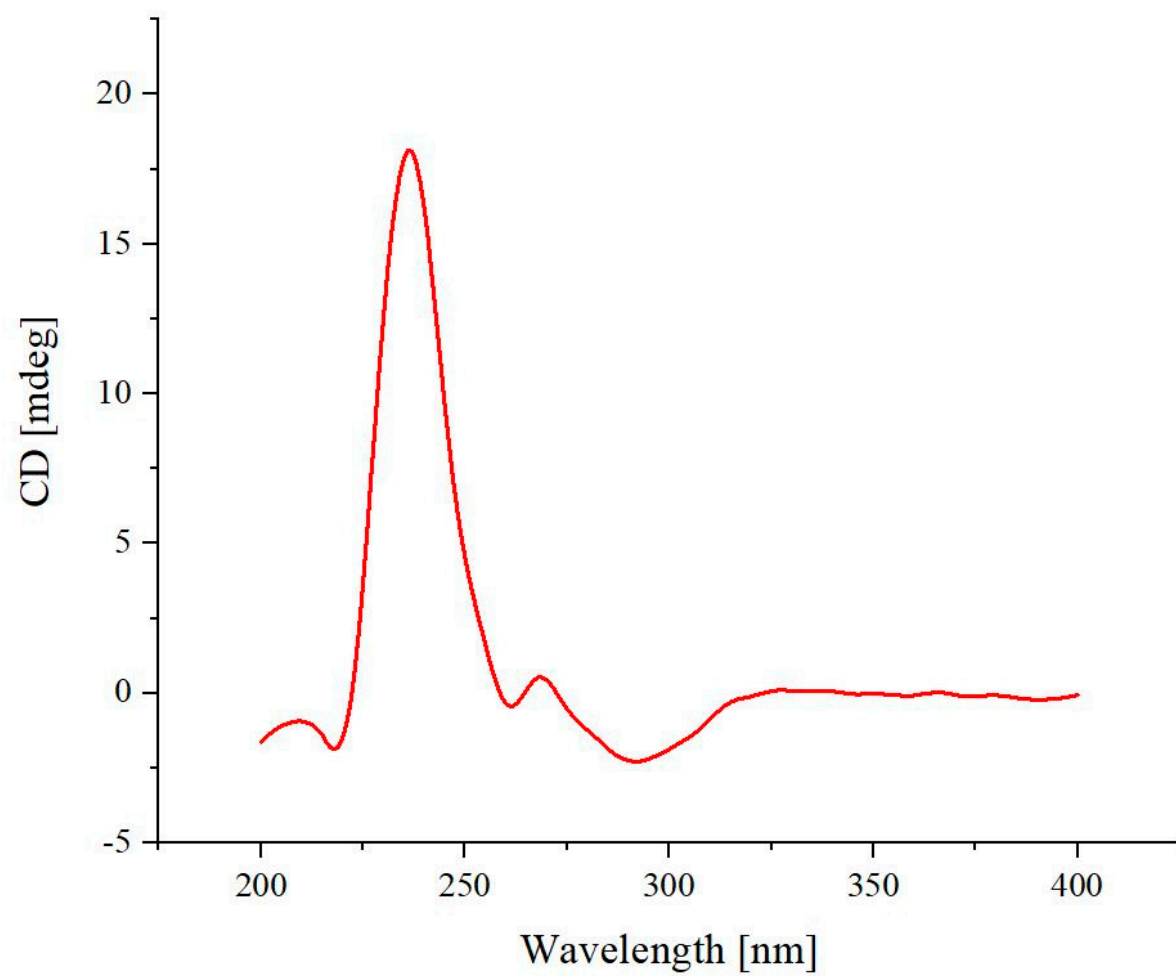


Figure S34. CD spectrum of **3** in MeOH.

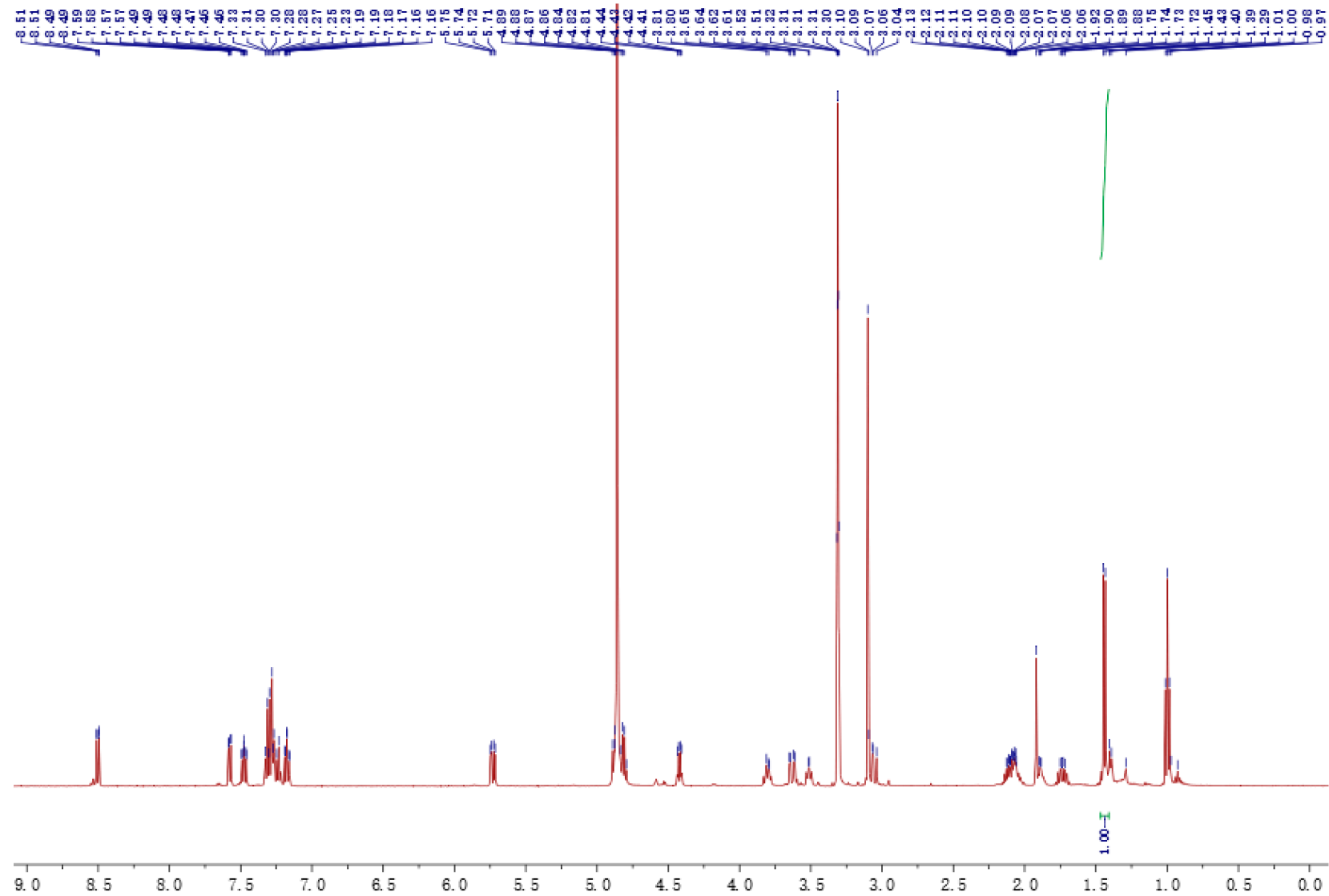


Figure S35.  $^1\text{H}$  NMR ( $\text{CD}_3\text{OD}$ , 500 MHz) spectrum of **4**.

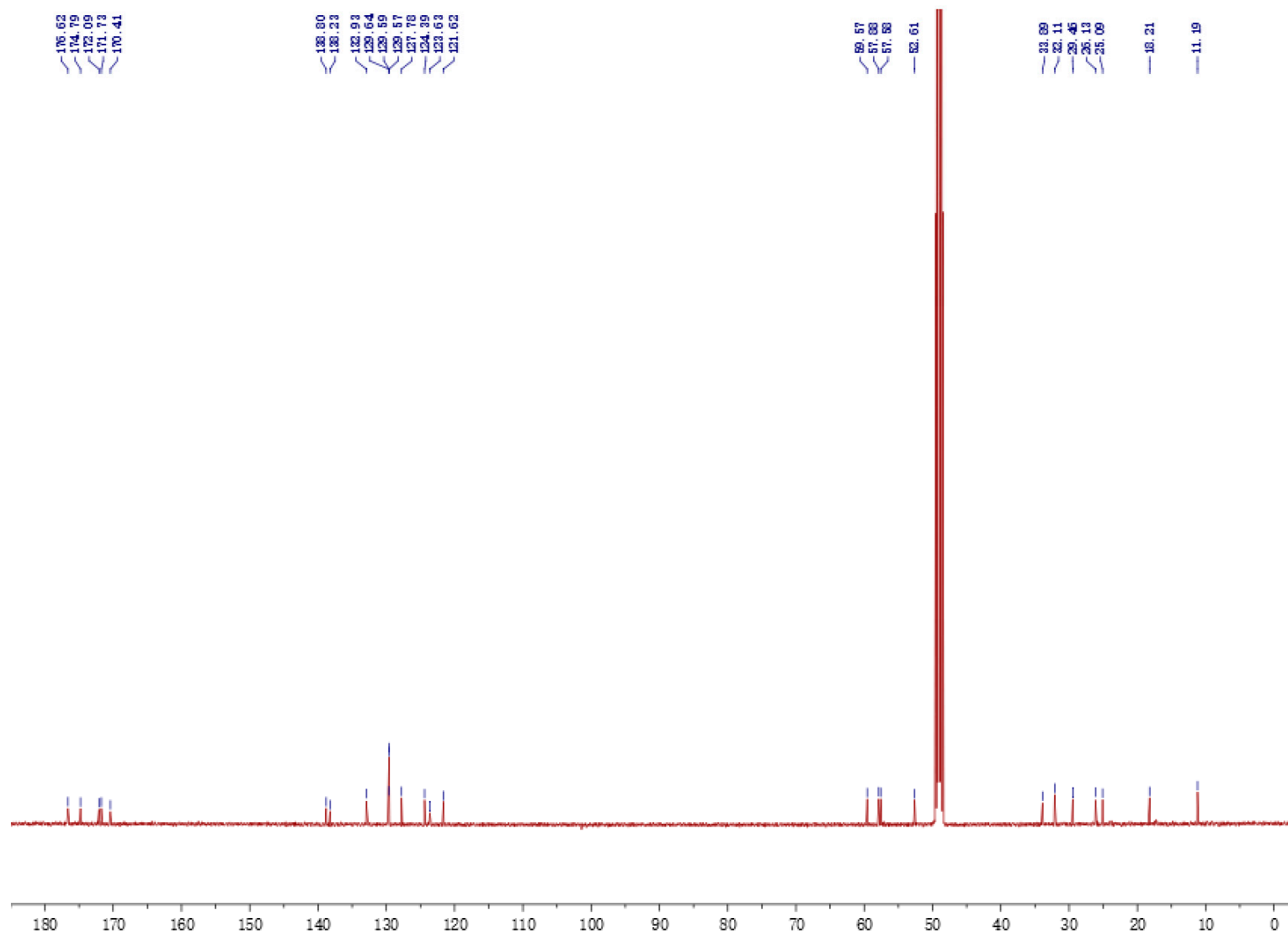


Figure S36.  $^{13}\text{C}$  NMR ( $\text{CD}_3\text{OD}$ , 125 MHz) spectrum of **4**.

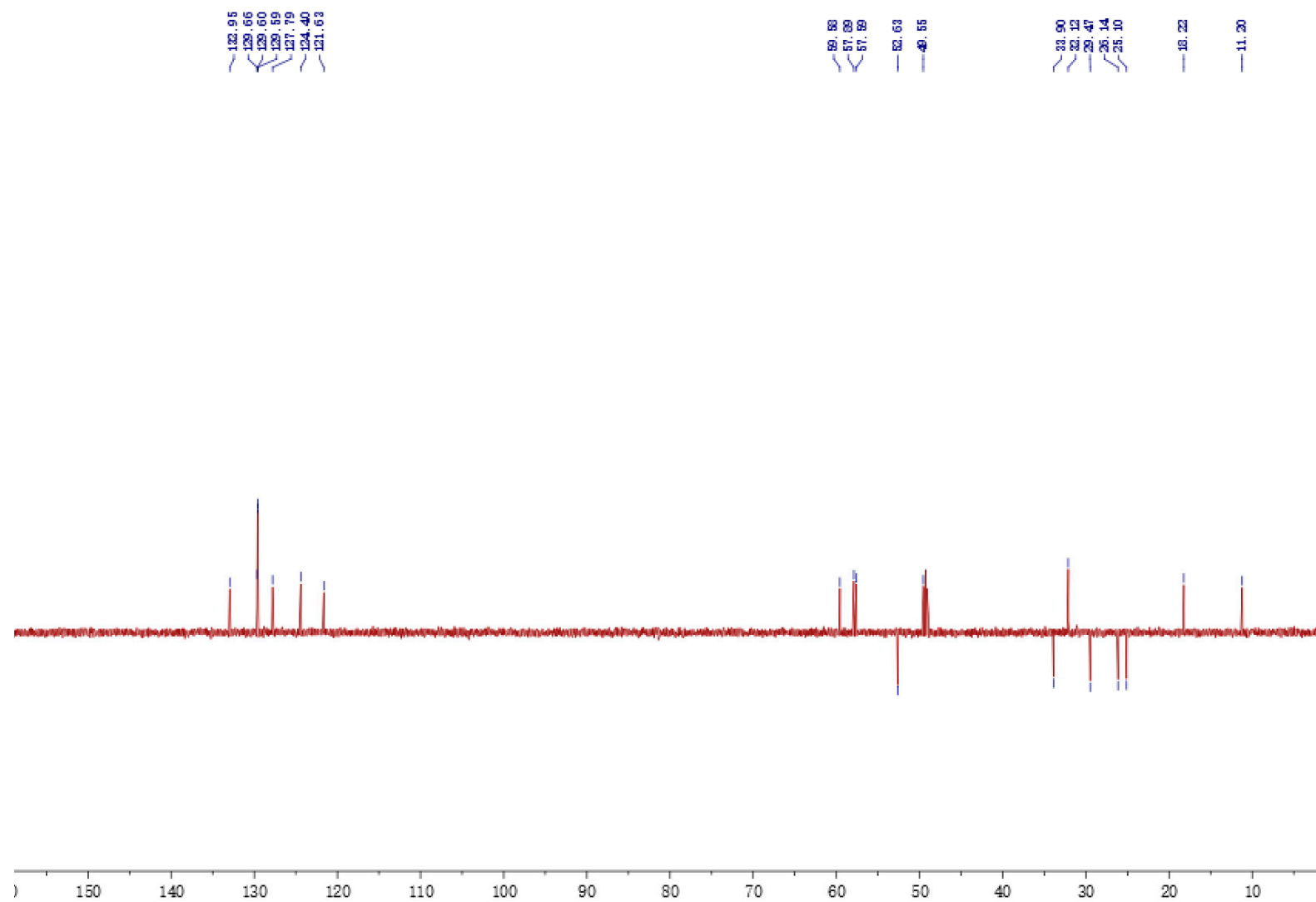


Figure S37. DEPT (CD<sub>3</sub>OD, 125 MHz) spectrum of 4.



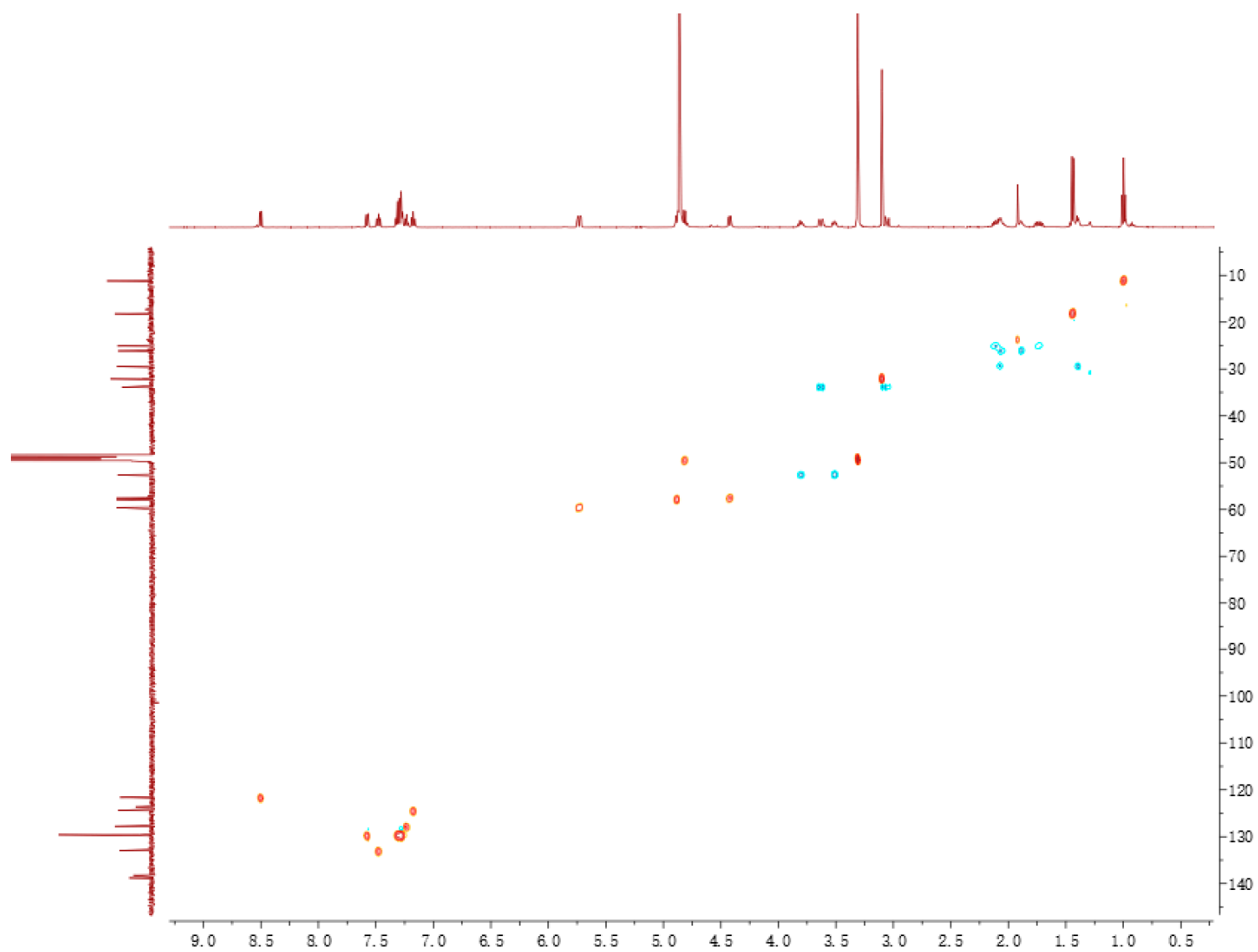


Figure S38. HMQC spectrum of **4**.

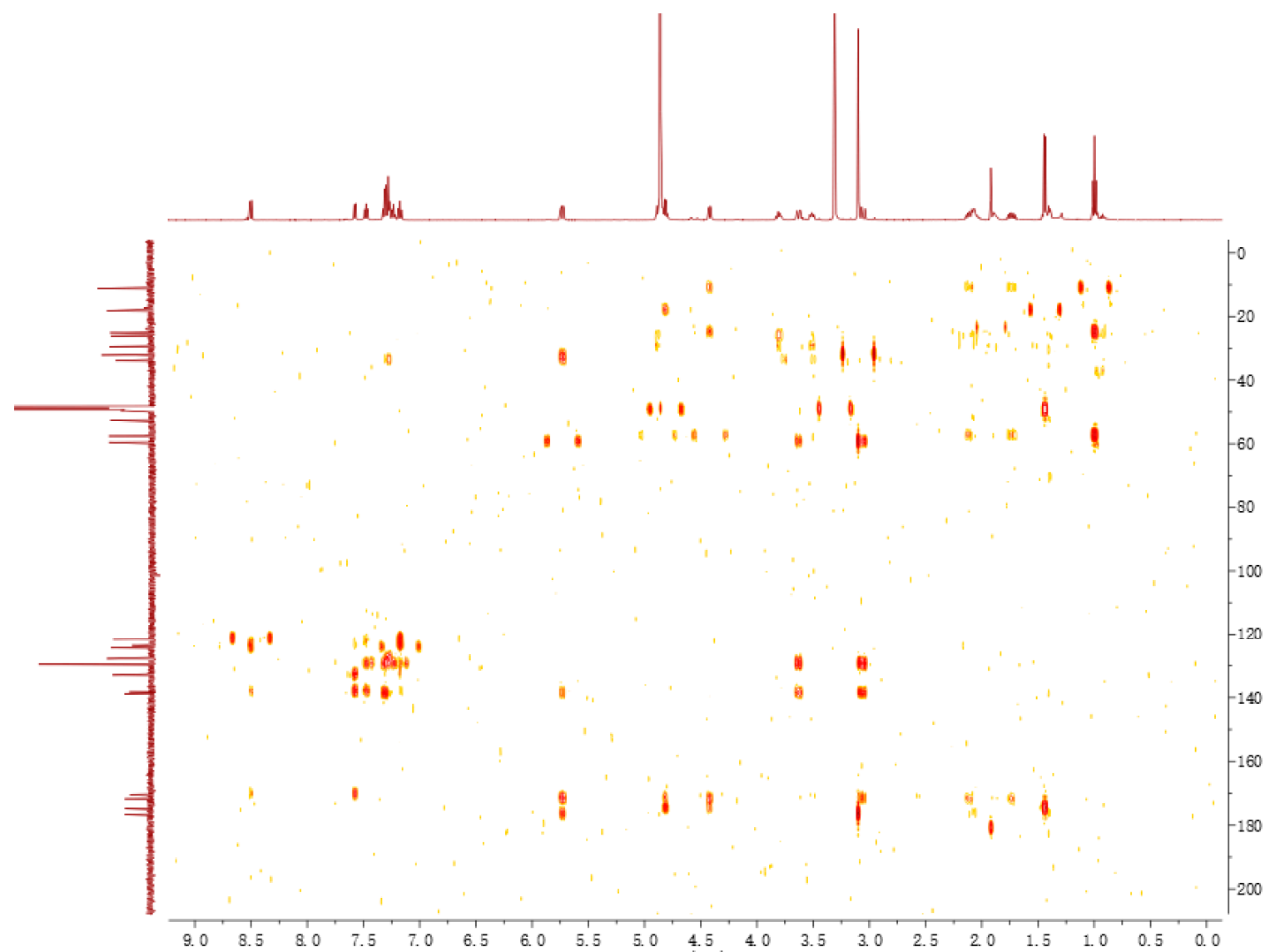


Figure S39. HMBC spectrum of **4**.

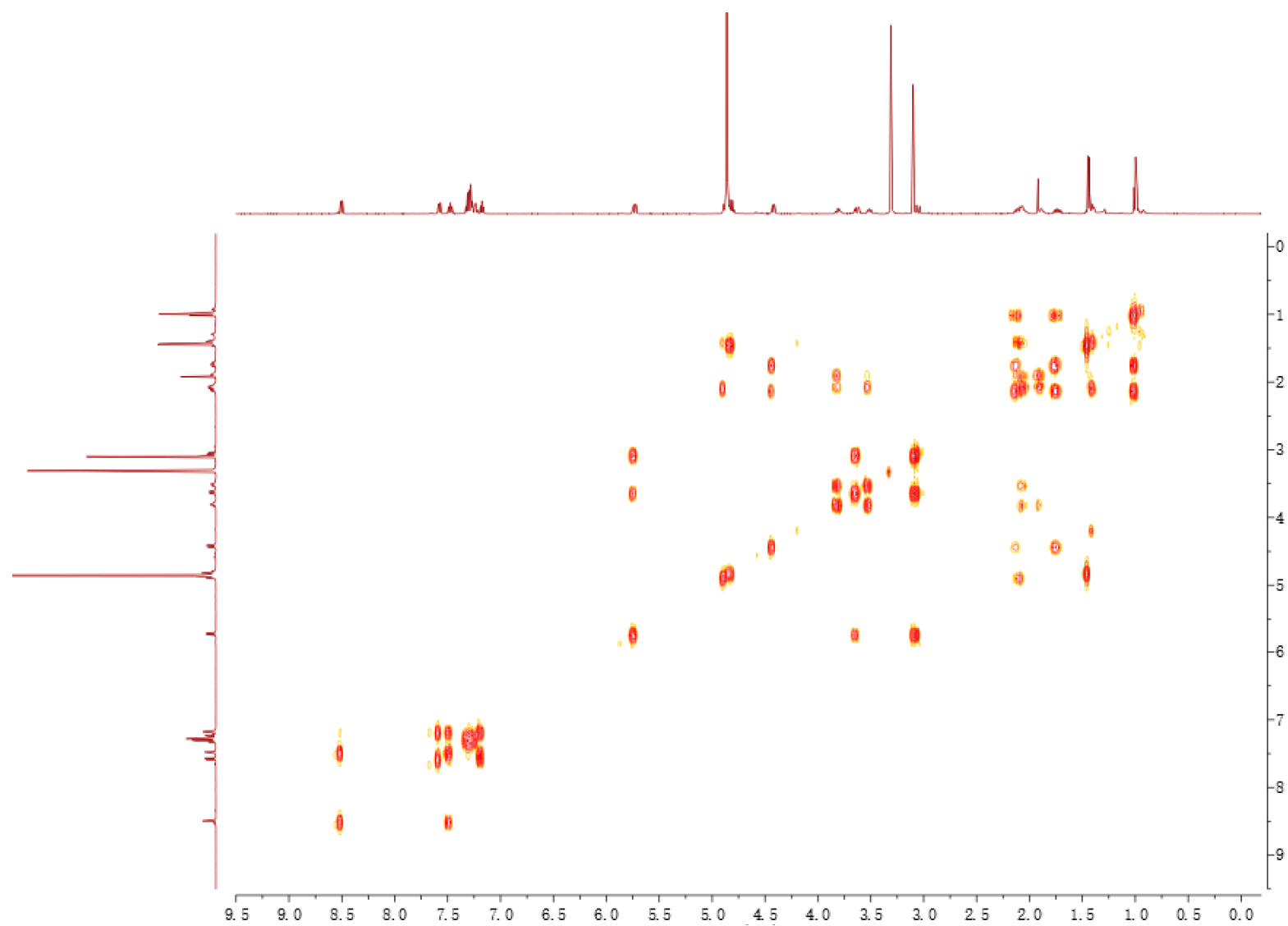


Figure S40.  $^1\text{H}$ - $^1\text{H}$  COSY spectrum of **4**.

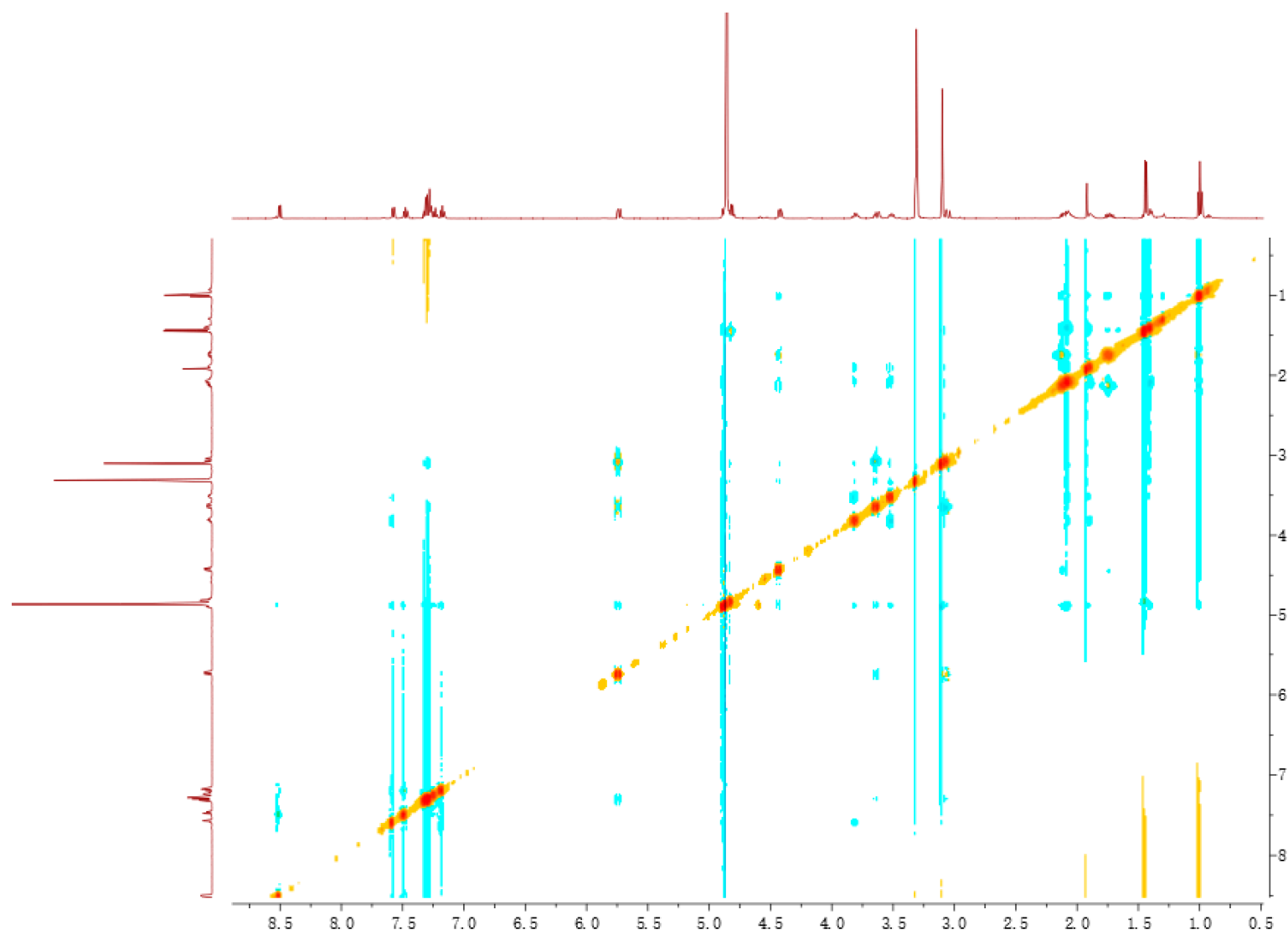


Figure S41. NOESY spectrum of **4**.

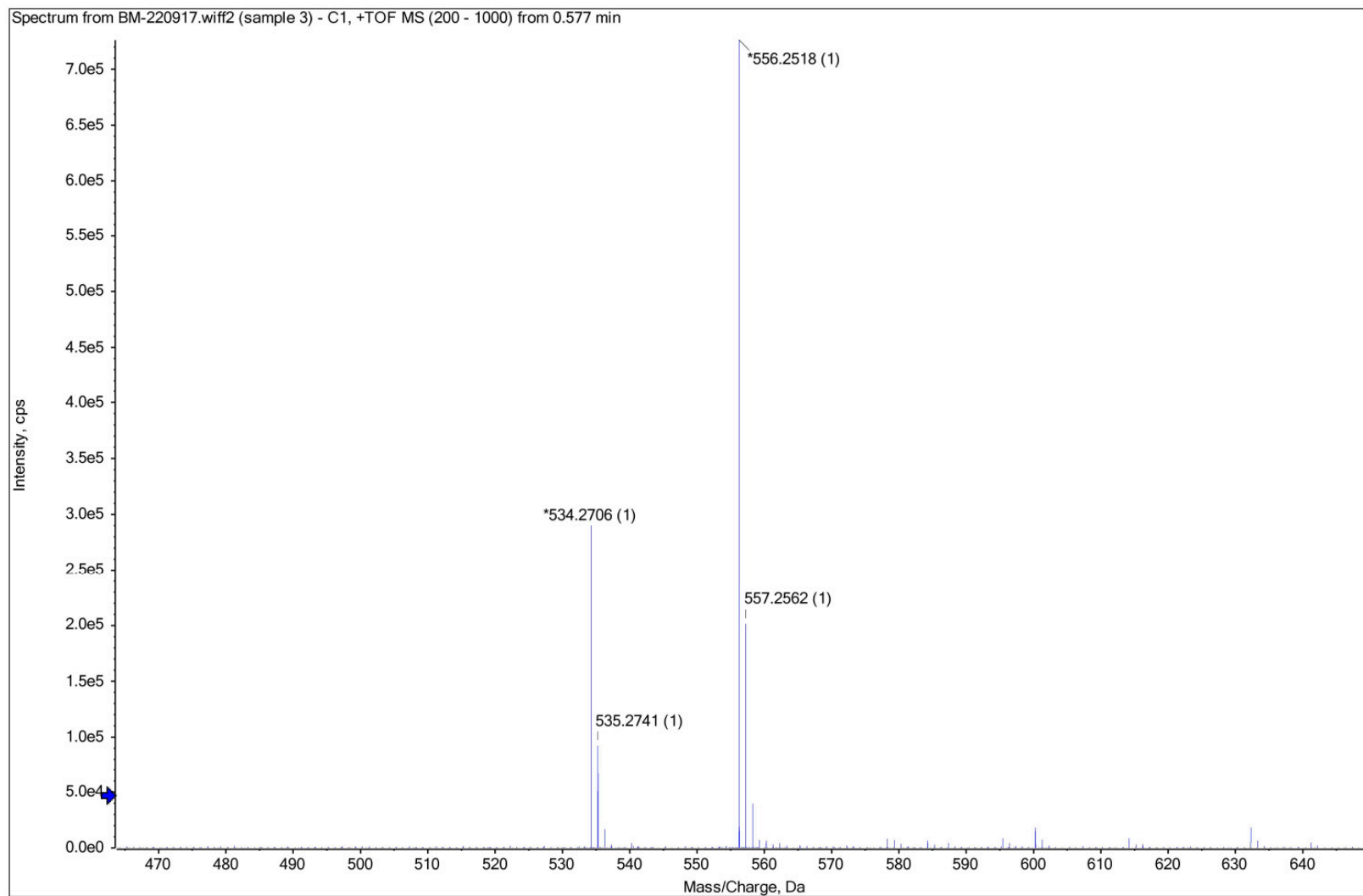


Figure S42. HR-ESI-MS spectrum of **4**.

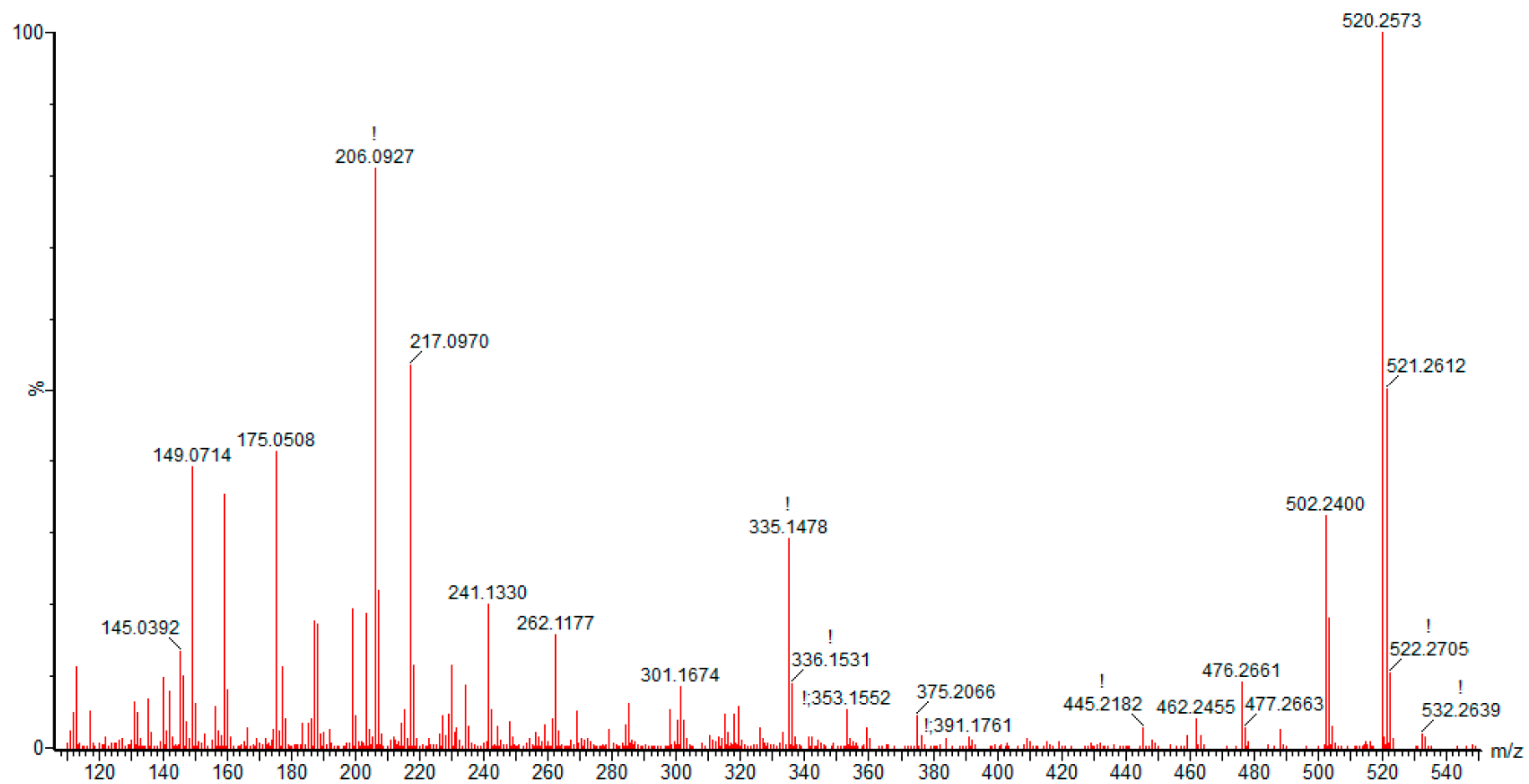


Figure S43. ESI-MS/MS spectrum of 4.

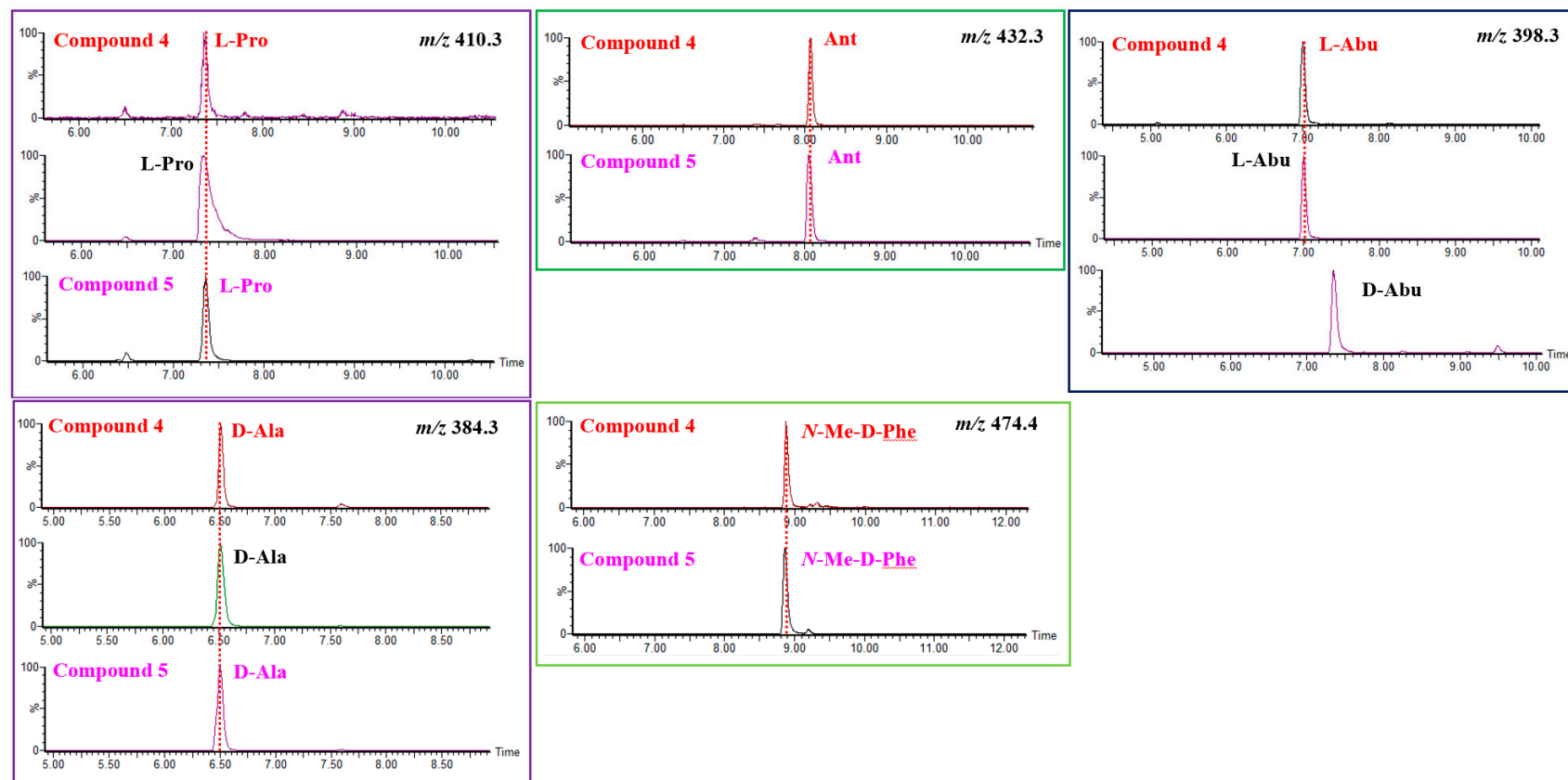


Figure S44. Marfey's analysis of **4**.

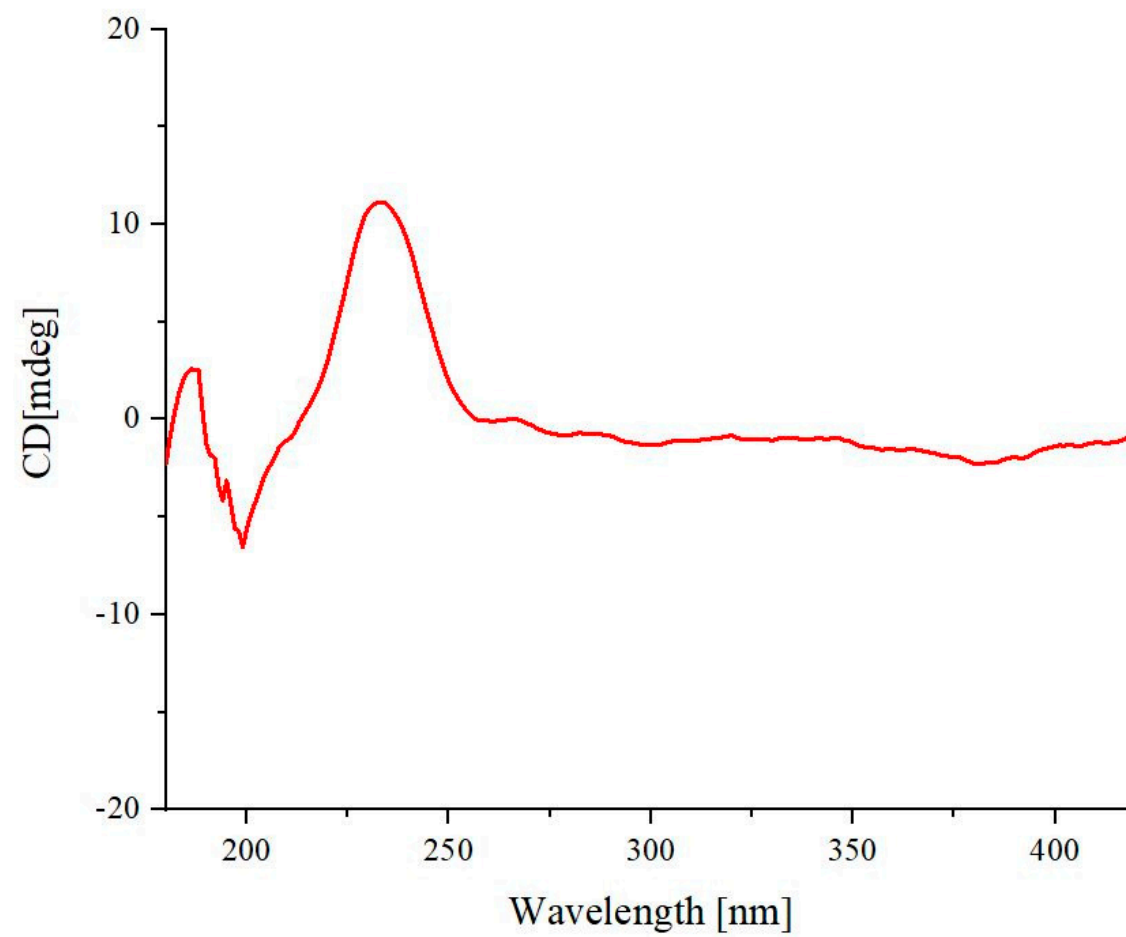
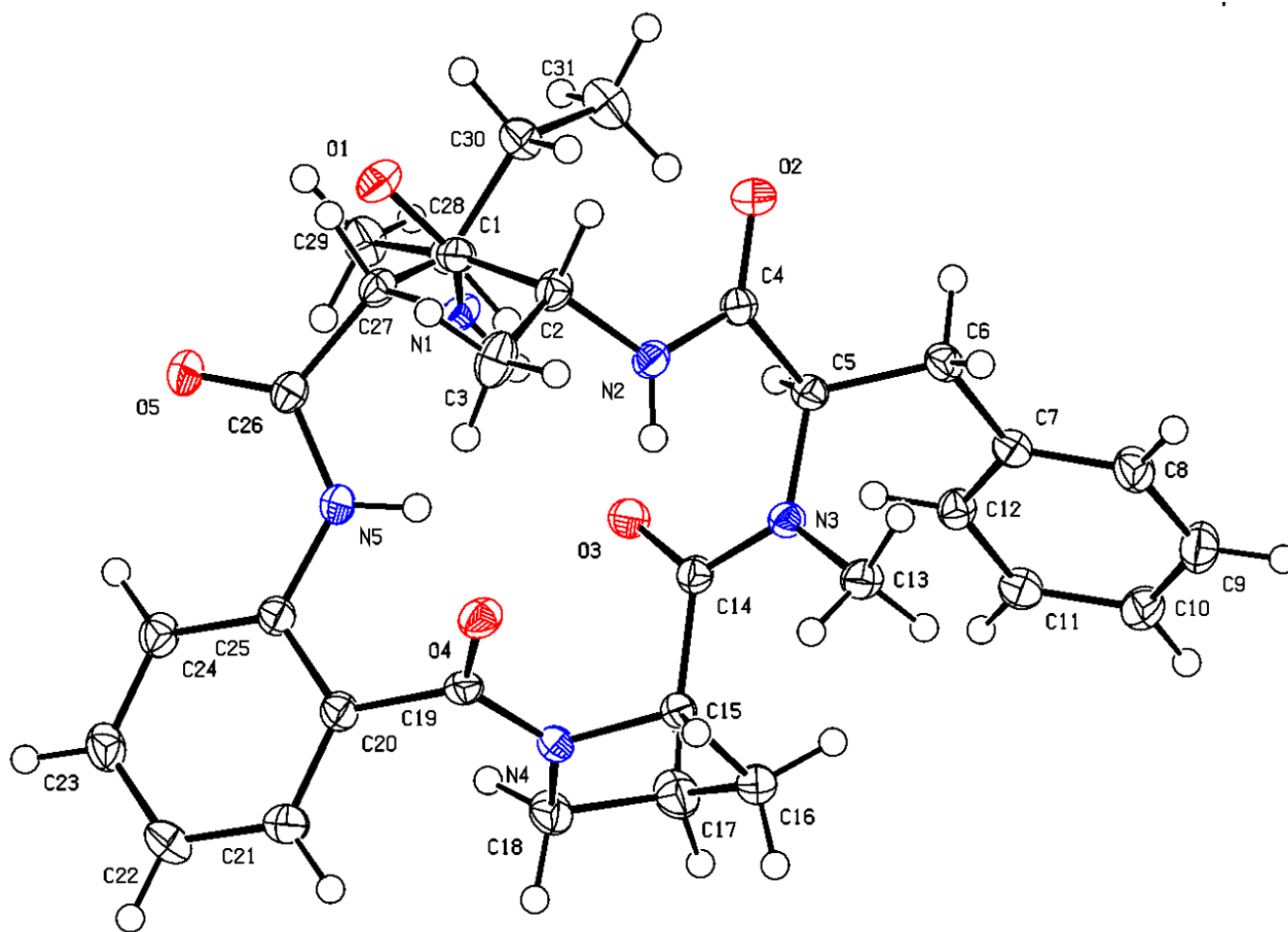


Figure S45. CD spectrum of **4** in MeOH.



Crystal data and structure refinement for 5



Empirical formula	C <sub>31</sub> H <sub>39</sub> N <sub>5</sub> O <sub>5</sub>
Formula weight	561.67
Temperature/K	99.9(3)
Crystal system	monoclinic
Space group	P2 <sub>1</sub>
a/Å	7.82520(10)
b/Å	18.63970(10)
c/Å	10.36950(10)
α/°	90
β/°	107.4970(10)
γ/°	90
Volume/Å <sup>3</sup>	1442.51(3)
Z	2
Q <sub>calc</sub> /g/cm <sup>3</sup>	1.293
μ/mm <sup>-1</sup>	0.721
F(000)	600.0
Crystal size/mm <sup>3</sup>	0.3 × 0.25 × 0.2
Radiation	Cu Kα (λ = 1.54184)
2Θ range for data collection/°	8.942 to 148.786
Index ranges	-9 ≤ h ≤ 9, -22 ≤ k ≤ 23, -11 ≤ l ≤ 12
Reflections collected	26446
Independent reflections	5709 [R <sub>int</sub> = 0.0242, R <sub>sigma</sub> = 0.0132]
Data/restraints/parameters	5709/1/375
Goodness-of-fit on F <sup>2</sup>	1.074
Final R indexes [I ≥ 2σ (I)]	R <sub>1</sub> = 0.0274, wR <sub>2</sub> = 0.0713
Final R indexes [all data]	R <sub>1</sub> = 0.0274, wR <sub>2</sub> = 0.0714
Largest diff. peak/hole / e Å <sup>-3</sup>	0.16/-0.24
Flack parameter	0.06(6)